MABS
2021, VOL. 13, NO. 1, e1859049 (19 pages)
https://doi.org/10.1080/19420862.2020.1859049

Taylor & Francis
Taylor & Francis Group

REPORT

OPEN ACCESS Check for updates

Bispecific antibody target pair discovery by high-throughput phenotypic screening using in vitro combinatorial Fab libraries

Pallavi Bhatta[a], Kevin D. Whale[b], Amy K. Sawtell[b], Clare L. Thompson[c], Stephen E. Rapecki[a], David A. Cook[b], Breda M. Twomey[b], Milena Mennecozzi[b], Laura E. Starkie[a], Emily M. C. Barry[a], Shirley J. Peters[a], Ahmad M. Kamal[d], and Helene M. Finney[b]

[a]New Modalities and Therapeutics Group, UCB Pharma, Slough, Berkshire UK; [b]In Vitro Pharmacology Group, UCB Pharma, Slough, Berkshire, UK; [c]Immunology Research Group, UCB Pharma, Slough, Berkshire UK; [d]Immunology Partnering Group, UCB Pharma, Slough, Berkshire UK

ABSTRACT

Bispecific antibodies can uniquely influence cellular responses, but selecting target combinations for optimal functional activity remains challenging. Here we describe a high-throughput, combinatorial, phenotypic screening approach using a new bispecific antibody target discovery format, allowing screening of hundreds of target combinations. Simple *in vitro* mixing of Fab-fusion proteins from a diverse library enables the generation of thousands of screen-ready bispecific antibodies for high-throughput, biologically relevant assays. We identified an obligate bispecific co-targeting CD79a/b and CD22 as a potent inhibitor of human B cell activation from a short-term flow cytometry signaling assay. A long-term, high-content imaging assay identified anti-integrin bispecific inhibitors of human cell matrix accumulation targeting integrins β1 and β6 or αV and β1. In all cases, functional activity was conserved from the bispecific screening format to a therapeutically relevant format. We also introduce a broader type of mechanistic screen whereby functional modulation of different cell subsets in peripheral blood mononuclear cells was evaluated simultaneously. We identified bispecific antibodies capable of activating different T cell subsets of potential interest for applications in oncology or infectious disease, as well as bispecifics abrogating T cell activity of potential interest to autoimmune or inflammatory disease. The bispecific target pair discovery technology described herein offers access to new target biology and unique bispecific therapeutic opportunities in diverse disease indications.

ARTICLE HISTORY
Received 31 August 2020
Revised 15 November 2020
Accepted 29 November 2020

KEYWORDS
Bispecific; antibody; target; discovery; high-throughput; phenotypic; screening

Introduction

Therapeutic antibodies are entering clinical development and gaining approval in record numbers.[1] Bispecific antibodies, designed to engage two distinct targets or target epitopes, potentially represent the next generation of antibody therapeutics. There are over 90 bispecific antibodies in development,[2] and 2 currently approved: emicizumab-kxwh (Hemlibra®), co-targeting factor IX and factor X for hemophilia A;[3] and blinatumomab (Blincyto®), a bispecific T cell engager (BiTE) co-targeting CD3 and CD19 for acute lymphoblastic leukemia.[4,5] These are "obligate bispecific antibodies" where function is dependent upon the physical linkage of two distinct binding specificities, facilitating access to biological functions that cannot be achieved with either parental antibody alone or a mixture of the antibodies. The majority of obligate bispecific antibodies in development serve to redirect effector T cells or natural killer (NK) cells to tumor-associated antigens in a range of cancers,[6] but alternative potential mechanisms and obligate bispecific concepts in addition to bridging cells (in *trans*) are also being explored, such as receptor activation (in *cis*), receptor inhibition (in *cis*), cofactor mimetics and piggybacking.[7]

Bispecific target selection to date has been largely hypothesis-driven; either by pre-selection of a defined antigen pair or a small number of functionally related targets, based on their known biological function. Although extensive functional screening of panels of bispecific antibodies has been reported to be necessary for optimal antibody selection for a given target pair,[8,9] a systematic, large-scale screening approach has not yet been fully exploited for the co-discovery of the optimal target antigen pairs for modulation of a given cellular response. The functional activity of bispecific antibodies, particularly those targeted to cell surface receptors, is difficult to predict from that of the individual parental antibodies. We propose high-throughput functional screening using diverse, combinatorial libraries of bispecific antibodies to find the optimum target pair and subsequently antibody pair, for modulation of any given disease-relevant cellular response. We have developed a bispecific screening format that enables simple generation and functional evaluation of hundreds of combinations of target specificities in high-throughput, disease-relevant human cell assays. Since antibodies that modulate receptor signaling are susceptible to geometric constraints,[10–12] this screening format, which we term Fab-K_D-Fab, is monovalent and contains highly flexible linkages. The Fab-K_D-Fab molecule is formed by *in vitro* mixing of two halves comprising Fab-fusion proteins, Fab-X and Fab-Y, where X and Y form a non-covalent heterodimeric

CONTACT Pallavi Bhatta. Pallavi.Bhatta@ucb.com
Supplemental data for this article can be accessed on the publisher's website.

association of sufficient affinity and stability to enable high-throughput screening in both short- and long-term complex human cell-based assays. Importantly, the Fab-K_D-Fab is Fc-free to enable direct assessment of the effects of bispecific targeting, without interference from Fc-driven activity, particularly in assays using heterogenous immune cell populations.

We have evaluated our bispecific screening technology across various mechanism-based disease-relevant phenotypic *in vitro* models, and describe here three distinct applications using very different screening approaches utilizing human primary cells. Firstly, we describe the identification of a potent, obligate bispecific inhibitor of B cell receptor (BCR) function to target aberrant B cell activity characteristic of autoimmune diseases such as systemic lupus erythematosus (SLE).[13] This molecule was discovered in a high-throughput, short-term, human peripheral blood mononuclear cells (PBMC)-based flow cytometry signaling assay designed to mimic the B cell hyper-reactivity observed in SLE patients. By screening 1992 Fab-K_D-Fab bispecific antibodies encompassing 23 targets and 300 different target combinations, we identified a bispecific antibody co-targeting CD79a/b and CD22, which was a potent inhibitor of a range of B cell functions. This functional activity was entirely dependent upon the molecule being a bispecific, as activity was not replicated by the single parental antibodies or a mixture of these antibodies.

Secondly, we describe the identification of potent bispecific inhibitors of extracellular matrix (ECM) accumulation, directed against target antigens in a coculture of human primary lung epithelial cells and lung fibroblasts. Excessive accumulation of ECM is a hallmark feature of fibrotic disease, which is recapitulated in the coculture screen mimicking the characteristics of fibrotic tissue remodeling and ECM accumulation in a 7 d, high-throughput, high-content imaging assay.[14,15] By screening 1671 Fab-K_D-Fab bispecific antibodies encompassing 23 targets and 239 different target combinations, we identified a bispecific antibody co-targeting the β1 and β6 integrins, which showed obligate bispecific-dependent inhibition of fibronectin accumulation and additive bispecific-dependent inhibition of collagen I and III accumulation. In addition, we identified a bispecific antibody co-targeting the αV and β1 integrins, which showed considerably more potent inhibition of ECM accumulation compared to the αV integrin bivalent parental antibody.

In both of these screens, the primary hits were further confirmed and validated in secondary assays using a molecularly linked BYbe™ format[16] and a bispecific IgG format in the case of CD79a/b-CD22. The discovery of these new bispecific target pairs for different disease-relevant phenotypes demonstrates the utility of the Fab-K_D-Fab screening format in assays modeling complex biology in human primary cells. Moreover, this approach shows the value of larger, less hypothesis-driven bispecific target discovery to exploit the unique therapeutic opportunities that bispecific antibody therapies can potentially deliver.

In this respect, our third screen demonstrates how larger screens of PBMC functional modulation can be executed to address broader mechanistic questions with data simultaneously captured for both the activation and inhibition of multiple end points from diverse cellular subsets under different stimulation conditions. The screen we describe focused on the activation of different T cell subsets and soluble mediators within a PBMC population, but this screen can easily be adapted by changing the stimuli, target cell subset(s), activation markers and soluble mediators measured to explore different mechanisms of interest. We assessed the effect of bispecific antibodies under three different stimulation conditions on four activation markers, covering seven unique cell subsets in addition to quantification of three soluble mediators. Although our immediate interest was in bispecifics that activated T cells, the screen was purposely designed to further capture bispecific T cell inhibitors for future potential interest with respect to autoimmune or inflammatory disease. We screened 6417 Fab-K_D-Fab bispecific antibodies encompassing 49 targets and 969 different target combinations using PBMC from 2 independent donors. Here we illustrate a "snapshot" of the diversity of bispecific antibodies identified that either enhanced or inhibited T cell activity.

Results

Generation of the Fab-K_D-Fab bispecific antibody screening format

To facilitate the generation of large bispecific antibody libraries, two Fab-fusion proteins, Fab-X (Fab-scFv) and Fab-Y (Fab-peptide), were designed based on the reported strong-affinity antibodies to a peptide derived from the yeast transcription factor GCN4.[17] This antibody (52SR4) and target (GCN4 peptide) combination was selected based on three key criteria relating to the target: (1) it is not expressed in human cells, (2) the epitope is linear, and (3) it has a very slow dissociation rate from the antibody. The Fab is fused to either 52SR4 scFv (X) or GCN4 peptide (Y) (Figure 1a). Fab-X and Fab-Y proteins with specificities toward a range of target antigens were expressed transiently as C-terminally His-tagged proteins. The expression level of the Fab-X in the cell culture supernatant typically ranged from 50 to 250 μg/mL, whereas the expression level of the Fab-Y typically ranged from 100 to 400 μg/mL. Proteins were immobilized metal affinity chromatography (IMAC) purified, and the purified proteins were analyzed by sodium dodecyl sulfate-polyacrylamide gel electrophoresis (SDS-PAGE) and size exclusion ultra-performance liquid chromatography (SE-UPLC); representative data are shown in Figure S1 and Figure 1. The reducing SDS-PAGE gel (Figure S1) shows banding patterns that indicated the constructs were being expressed correctly, with bands at approximately 50 kDa and 25 kDa (Fab-X) or a doublet at approximately 25 kDa (Fab-Y). Fab-X and Fab-Y proteins were highly monomeric following a one-step affinity purification, typically displaying monomer levels of approximately 90% and over 95%, respectively (Figure 1b).

Exploiting the reported strong-affinity interaction between 52SR4 scFv (X) and the GCN4 peptide (Y),[17] the bispecific screening format was made by mixing the Fab-X and Fab-Y *in vitro* in a 1:1 molar ratio to allow complex

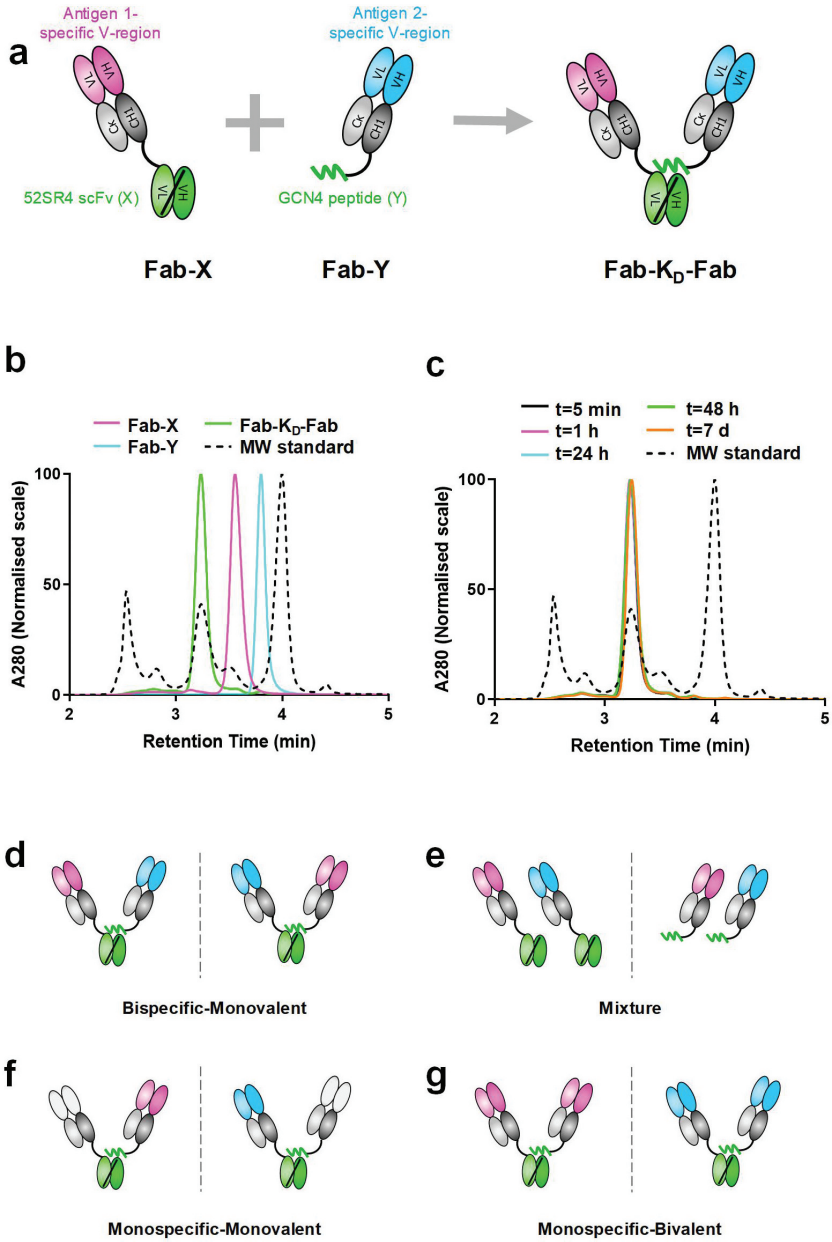

Figure 1. Generation of the Fab-K$_D$-Fab bispecific screening format. (a) The Fab-K$_D$-Fab bispecific complex is formed by *in vitro* mixing of two Fab-fusion proteins, Fab-X and Fab-Y, where X is a scFv with strong binding affinity for peptide Y. (b) Representative SE-UPLC data of a Fab-X, Fab-Y and Fab-K$_D$-Fab following mixing of the Fab-X and Fab-Y in a 1:1 molar ratio in PBS, pH7.4. Peak heights are normalized to 100%. (c) SE-UPLC analysis of the Fab-K$_D$-Fab complex following incubation at 37°C in PBS, pH7.4 for 5 min, 1 h, 24 h, 48 h and 7 d. Peak heights are normalized to 100%. Gel filtration protein standards were loaded for molecular weight estimation. (d) Generation of bispecific-monovalent Fab-K$_D$-Fabs (Fab1-X + Fab2-Y; or Fab2-X + Fab1-Y); (e) Fab mixture controls (Fab1-X + Fab2-X; or Fab1-Y + Fab2-Y); (f) Generation of monospecific-monovalent Fab-K$_D$-Fab controls (Negative Fab-X + Fab1-Y; or Fab2-X + negative Fab-Y); (g) Generation of monospecific-bivalent Fab-K$_D$-Fab controls (Fab1-X + Fab1-Y; or Fab2-X + Fab2-Y).

formation (Figure 1a). The resulting Fab-K$_D$-Fab complexes were highly pure after mixing (Figure 1b); therefore, no further purification or processing steps were required. SE-UPLC analysis showed that the Fab-X and Fab-Y complexed within minutes of mixing, and were stable at 37°C, with Fab-K$_D$-Fab integrity remaining unchanged over 7 d (Figure 1c). The Fab-K$_D$-Fab bispecific antibody format is therefore highly pure and stable, and thus amenable to high-throughput screening in both short- and long-term functional assays.

Bispecific screen for inhibitors of BCR signaling

Cross-linking the BCR on mature B cells leads to rapid induction of downstream signaling events. The rapid coordinated action of Src family kinases on CD79a and CD79b intracellular domains leads to their phosphorylation and activates Syk, which in turn activates multiple downstream partners such as PLCγ2 and BTK.[18] BCR signals then integrate with signals from associated regulatory molecules (e.g., CD19 and CD22) leading to modulation of Akt, calcium flux and NF-κB,[19] which

activate or inhibit B cell activity in a context-dependent fashion. These responses are subsequently additionally fine-tuned by members of the MAP kinase family such as p38 and Erk1 and 2.[20] In autoimmunity, many of these signaling pathways are altered and can contribute directly and indirectly to the disease state.[21] Aberrant BCR signaling has been implicated in the selection and survival of B cells, B cell tolerance, germinal center reactions and the generation of short-lived plasmablasts, all of which can contribute to autoimmunity.[21] To assess the contribution of BCR signaling in the context of an autoimmune disease, we measured signaling readouts downstream of the BCR in SLE patients and compared these with healthy individuals. In order, to encompass the whole of the BCR signaling pathway we chose to measure the key signaling nodes Syk, Akt, NF-κB and Erk1/2. When compared to healthy volunteers, SLE patient samples showed a greater activation of all parts of the BCR pathway measured, seen as increased protein phosphorylation by flow cytometry (Figure 2). Using this information, we sought to develop a high-throughput human B cell signaling assay that mimicked the elevated signaling in SLE patients. To do this, we activated healthy naïve B cells within PBMC using an anti-IgM polyclonal antibody, which activated the same signaling proteins measured in SLE patients. We then screened bispecific antibodies to B cell surface antigens to identify novel bispecific target combinations that inhibited BCR activation. Key readouts of the upstream BCR pathway (phosphorylated Syk, PLCγ2 and Akt) were chosen for primary screening as they gave robust assay signals at the same activation time-point. Additional readouts such as phosphorylated NF-κB and p38 were used for follow-on studies to give further pathway coverage.

To generate Fab-X and Fab-Y libraries, target antigens were selected based on their expression on B cells or other immune cells that are likely to contribute to B cell function. Antibodies were made to a total of 23 different antigens and between 1 and 8 unique V-regions to each antigen were selected for screening from different V-region sequence families, based purely on their ability to bind PBMC as a Fab-Y. We deliberately did not pre-select antibodies of defined affinity, activity, or epitope to enable unbiased bispecific discovery, driven entirely by the functional cellular activity of the V-region combination. Fab-X and Fab-Y antibodies covering these 23 unique B cell antigens were purified and mixed to generate 1992 Fab-K_D-Fab molecules for screening in the B cell signaling assay. In total, bispecific antibodies encompassing 300 antigen combinations were screened. A Ward's clustered[22] heat map of the average percentage inhibition of intracellular phosphorylated Akt, PLCγ2 and Syk (pAkt, pPLCγ2 and pSyk) in gated B cells was generated (Figure 3a). Each line in the clustered heat map represents a different Fab-K_D-Fab molecule. The cluster analysis was pruned to 30 clusters. In the most inhibitory cluster depicted at the bottom of the dendrogram and detailed in cluster 30 (Figure 3b), over 80% of the bispecific antibodies had specificity for CD79a/b (herein referred to as CD79) and CD22. A total of 24 different CD79-CD22 bispecifics were tested, comprising 3 different V-regions to CD79 with 8 different V-regions to CD22, which all showed greater than 50% inhibition of at least two different readouts. Although our interest in the context of SLE was to identify inhibitors of B cell signaling, the screen was designed in such a way to also capture agonists of B cell signaling to cover additional future interest in oncology or infectious disease. These agonists are depicted at the top of the heat map in Figure 3a and detailed in the first few clusters in Figure 3b, with the strongest agonists being in clusters 1–3.

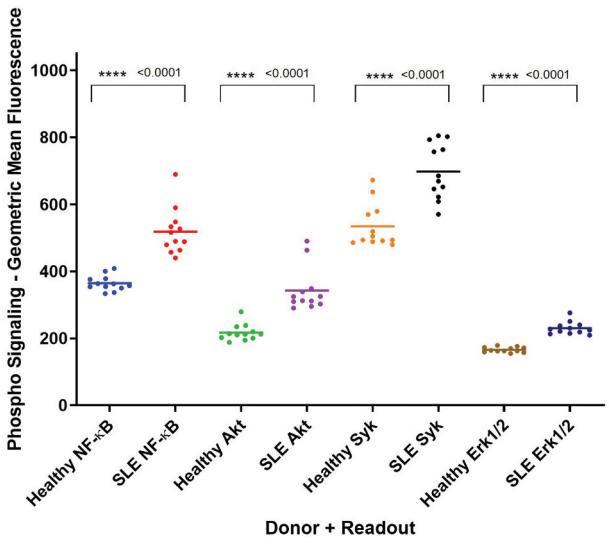

Figure 2. Intracellular signaling in SLE vs healthy PBMC. Intracellular signaling in unstimulated CD19$^+$ B cells from SLE patient PBMC compared to healthy individuals. The data are represented as geometric mean fluorescence values of intracellular phosphorylated protein expression for $n = 12$ donors in both cohorts and p-values calculated by a two-tailed unpaired t-test. Each dot represents the mean of three technical replicates from a single donor.

CD79-CD22 bispecific validation in the Fab-K_D-Fab format

To validate the CD79-CD22 hit identified in the B cell primary screen, a range of control Fab-K_D-Fab molecules were made. These included monospecific-monovalent Fab-K_D-Fab controls (Figure 1f) and monospecific-bivalent Fab-K_D-Fab controls (Figure 1g), which were made by complexing the two component Fab fusions, in the same way that the bispecific-monovalent Fab-K_D-Fab molecules (Figure 1d) were formed. The monospecific-monovalent Fab-K_D-Fab (Figure 1f) incorporated an inactive (negative binding) Fab-X or Fab-Y. Antibody mixture controls (Figure 1e) were also included during hit validation; either two Fab-X molecules or two Fab-Y molecules, which are unable to form a Fab-K_D-Fab complex. Concentration–response studies were performed with the bispecific Fab-K_D-Fab molecules, alongside the monospecific-monovalent Fab-K_D-Fab controls as well as monospecific-bivalent Fab-K_D-Fab controls and Fab-Y mixture. Only the CD79-CD22 bispecifics markedly inhibited BCR signaling in B cells activated with anti-IgM (Figure 4). Both bispecific Fab-K_D-Fab orientations, CD79-CD22 (CD79 Fab-X-CD22 Fab-Y) and CD22-CD79 (CD22 Fab-X-CD79 Fab-Y), robustly inhibited pAkt (80–82%), pp38 (91%), pPLCγ2 (53–59%) and pNF-κB (94%), whereas the controls showed minimal inhibition of pAkt and pPLCγ2 specifically (<32%). The CD79-CD79 bivalent Fab-K_D-Fab and, to a lower extent, the CD79 monospecific-monovalent Fab-K_D-Fab demonstrated some inhibition of pp38 and pNF-κB, but with greatly

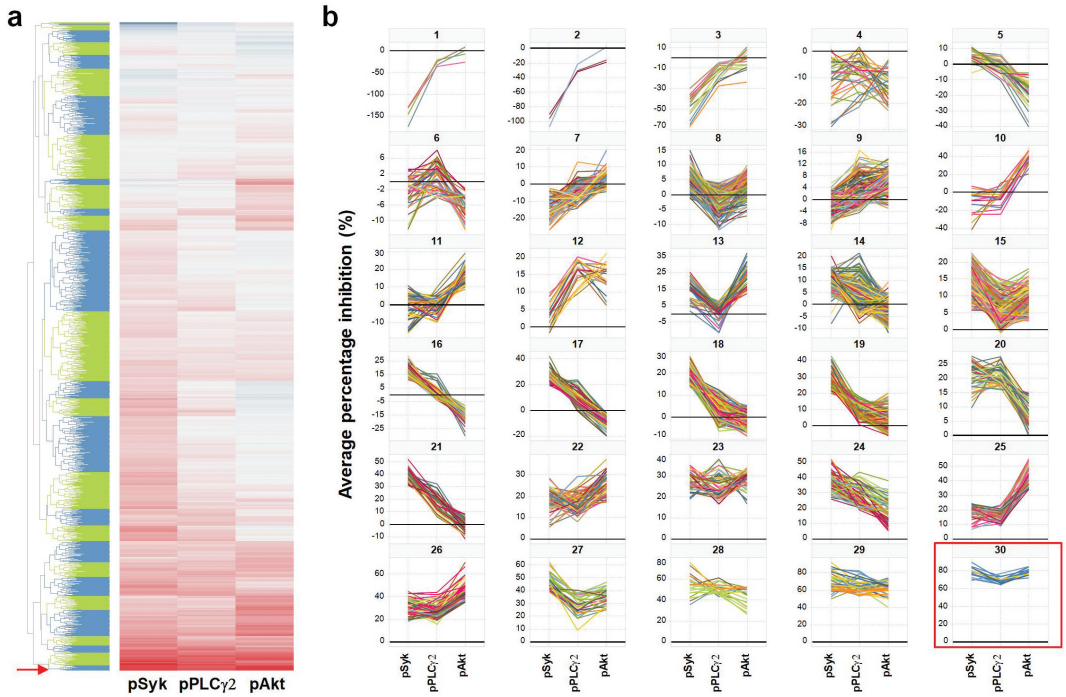

Figure 3. Identification of a CD79-CD22 bispecific inhibitor of BCR signaling from a primary B cell signaling screening assay. (a) Ward's clustered heatmap of B cell primary screen data for Fab-K_D-Fab molecules tested in 2 donors at a single concentration (200 nM) in the B cell signaling assay following anti-IgM stimulation of PBMC. Percentage inhibition of pAkt, pPLCγ2 and pSyk relative to anti-IgM and untreated controls are depicted. Red denotes inhibition of BCR activity (max 100% inhibition), blue denotes enhancement of BCR activity (max minus 180% inhibition) and gray denotes baseline (no effect on BCR activity). Each horizontal line represents a different Fab-K_D-Fab molecule. The cluster analysis was pruned to 30 clusters depicted in alternating blue and green on the dendrogram and the CD79-CD22 target pair selected from the most inhibitory bottom cluster (cluster 30). (b) Average percentage inhibition of pAkt, pPLCγ2 and pSyk for all Fab-K_D-Fab molecules in each of the 30 clusters defined in the dendrogram. Scale on Y-axis is defined for each cluster range covering 100% inhibition to minus 180% inhibition (activation). The cluster from which the CD79-CD22 target pair was selected (where greater than 50% inhibition was observed for all 3 parameters) is highlighted. Each horizontal line represents a different Fab-K_D-Fab molecule, and each color a different target combination.

reduced efficacy (<54%) compared to the bispecific molecules (91–94%). CD79 + CD22 Fab-Y mixtures showed minimal inhibition of all the readouts tested (<30%), demonstrating the obligate bispecific nature of this antigen pair, where the CD79 and CD22 Fabs must be linked for activity.

CD79-CD22 bispecific validation in the BYbe™ format

To demonstrate that the target pair biology identified in the Fab-K_D-Fab screening format is reproduced in a therapeutically relevant bispecific format, it was important to test the activity of the CD79-CD22 bispecific in a molecularly linked construct that has no potential to dissociate. To test this, we used the BYbe™ format,[16] which comprises a Fab (with specificity toward antigen 1) fused to a disulfide-stabilized scFv (with specificity toward antigen 2) via a G4S linker (Figure S2a). Bispecific-monovalent BYbe™ proteins were tested alongside monospecific-monovalent BYbe™ controls (comprising negative binding scFv), monospecific-bivalent BYbe™ controls and a negative BYbe™ control (comprising negative binding Fab and scFv) in the B cell signaling assay. BYbe™ schematics and SE-UPLC data for purified BYbe™ proteins are shown in Figure S2a. Similar concentration–response curves and IC_{50} values were obtained with the bispecific Fab-K_D-Fab and BYbe™ molecules, with the bispecific BYbe™ proteins consistently displaying a modest increase in potency compared to the bispecific Fab-K_D-Fab proteins (Figure 5, Table S1). In both bispecific BYbe™ orientations (CD79 Fab-CD22 scFv and CD22 Fab-CD79 scFv), robust inhibition of pAkt (82–86%), pp38 (88–91%), pPLCγ2 (58–-74%) and pNF-κB (92–94%) signaling was observed, which was equal to or moderately increased compared to the Fab-K_D-Fab. This increased inhibition is likely a result of physically linking the two antigen-binding specificities in the BYbe™ molecule. All other BYbe™ proteins showed minimal inhibition of these activation readouts, with the exception of the CD79-CD79 bivalent BYbe™ molecule. Analogous to the Fab-K_D-Fab format, the CD79-CD79 bivalent BYbe™ showed inhibition of pp38 and pNF-κB, but with reduced efficacy (50–54%) compared to the CD79-CD22 bispecific molecules (88–94%) (Figure 5, Table S1). The CD79-CD79 + CD22-CD22 bivalent BYbe™ mixture showed inhibition of activation readouts that were comparable to the CD79-CD79 bivalent molecule; thus, the activity observed with this mixture is likely attributed to the CD79-CD79 bivalent molecule. To further understand the differences in inhibition of B cell signaling by the CD79-CD22 bispecific and CD79-CD79 bivalent molecules, we tested their effects on B cell signaling in the absence of anti-IgM stimulation. Of all the BYbe™ proteins tested, only the CD79-CD79 bivalent BYbe™ protein and not the CD79-CD22 bispecific BYbe™ protein resulted in a concentration-dependent increase in pAkt (Figure S3), with no concomitant activation of PLCγ2, p38 or NF-κB (unpublished data). We hypothesize that the lack of bivalency for CD79 coupled to the specificity for

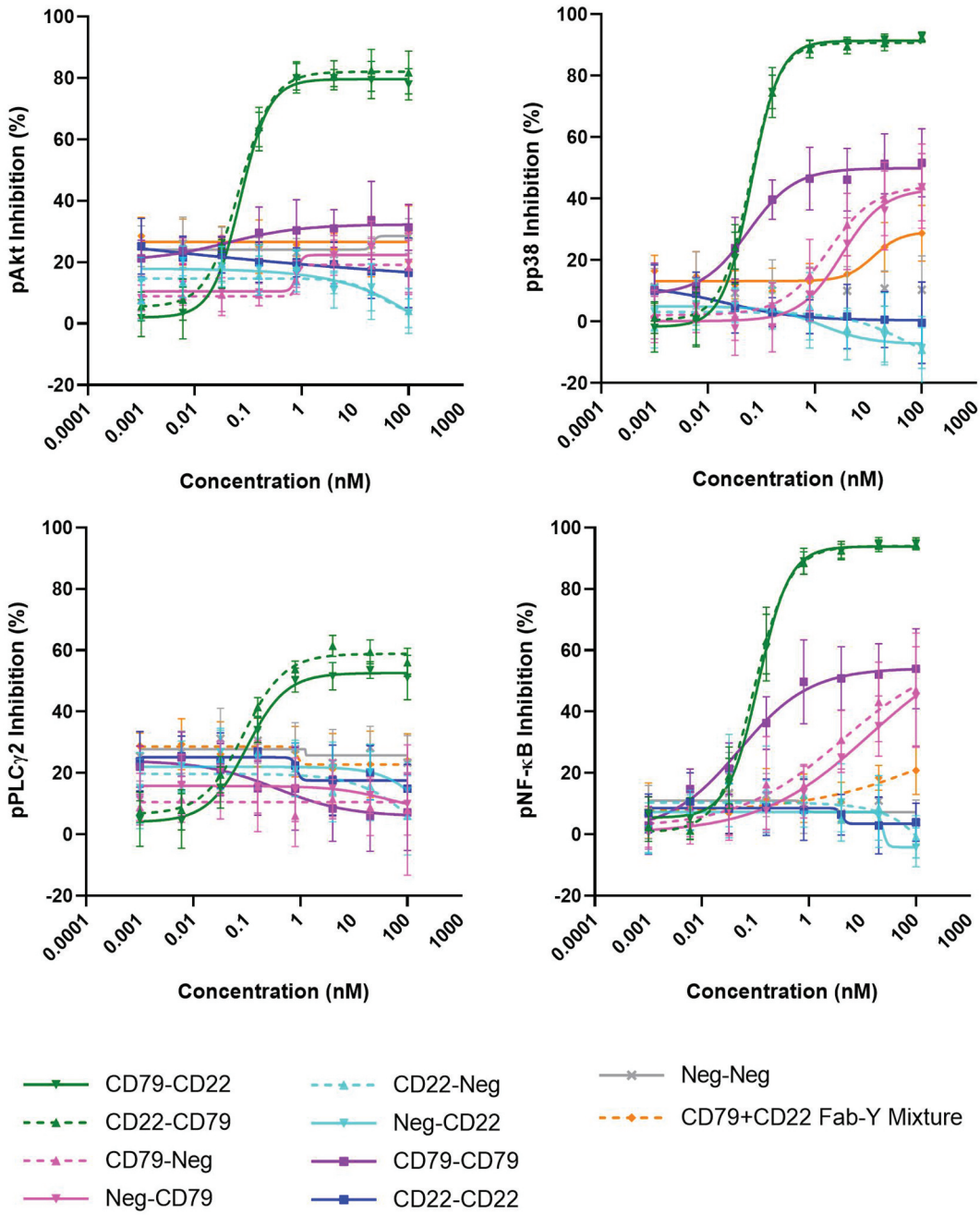

Figure 4. Validation of a CD79-CD22 bispecific inhibitor of BCR signaling from a primary B cell signaling screening assay. Assessment of CD79-CD22 bispecific Fab-K_D-Fabs alongside monospecific-monovalent Fab-K_D-Fabs, monospecific-bivalent Fab-K_D-Fabs and Fab-Y mixtures. 8-point concentration–response assays were performed in triplicate and pAkt, pp38, pPLCγ2 and pNF-κB levels were measured in B cells from the PBMC populations. Percentage inhibition values of pAkt, pp38, pPLCγ2 and pNF-κB relative to maximum and minimum control well data were calculated. Mean ± standard deviation of 6 donors are plotted.

CD22 in the bispecific BYbe^{TM} molecule overrides the capacity for CD79 targeting to induce B cell activation.[23]

Inhibition of B cell responses with a CD22-CD79 BYbe^{TM} and CD22-CD79 bispecific IgG

Following activation through the BCR, and with subsequent costimulation, B cells proliferate and differentiate, producing cytokines and antibodies that contribute to an ongoing immune response. After validation of CD79-CD22 bispecific BYbe^{TM} activity in the B cell signaling assay, we therefore evaluated the outcome of targeting these two antigens on additional B cell functional responses. Since the CD79-CD22 and CD22-CD79 BYbe^{TM} proteins previously gave comparable results, we selected one orientation, the CD22-CD79 BYbe^{TM}, and assessed inhibition of B cell proliferation, cell surface marker activation and cytokine production. Control CD79-CD79 and CD22-CD22 bivalent BYbe^{TM} proteins, or a mixture of the two, were also tested, as well as a negative control BYbe^{TM}. All molecules were tested at a final concentration of 100 nM, as this concentration gave maximum inhibition in all readouts of the B cell signaling assay (Figure 5). To

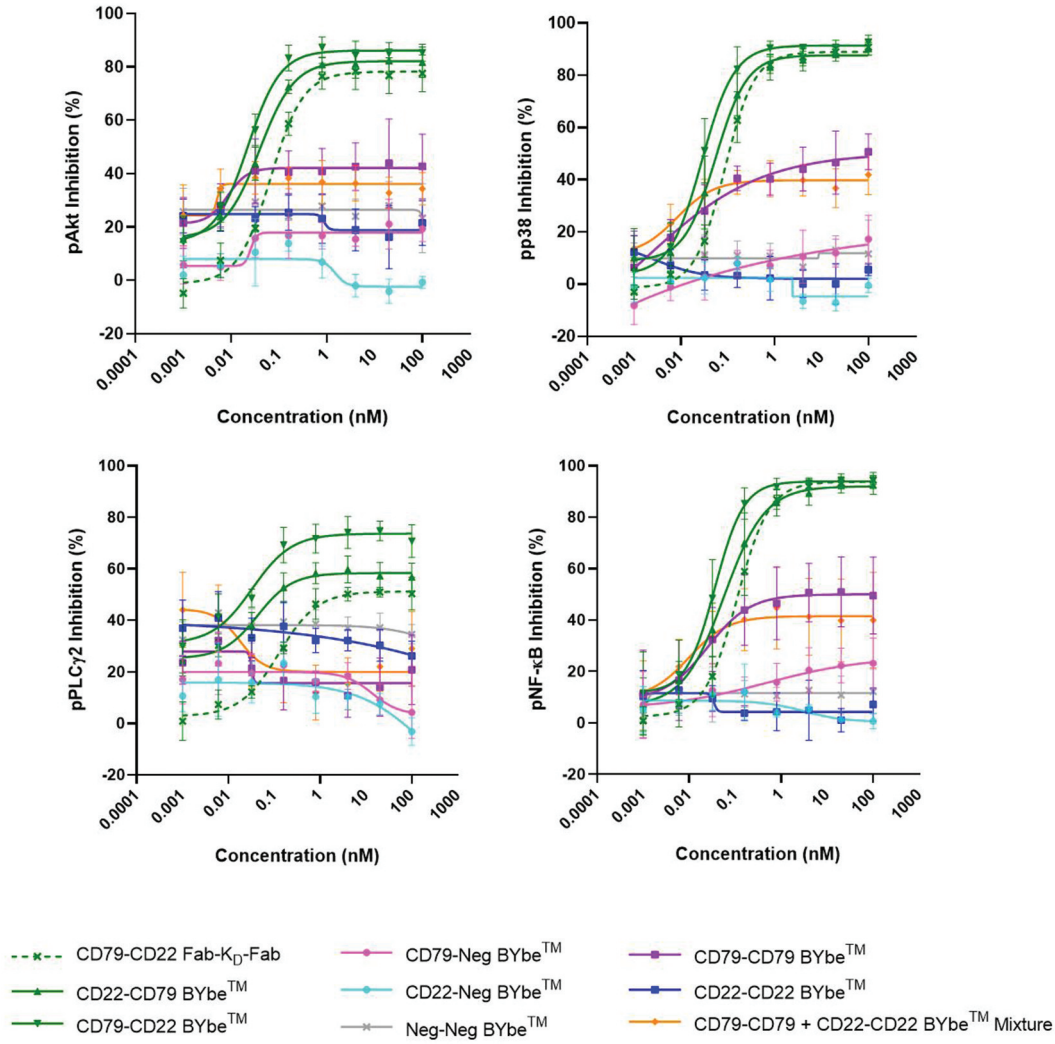

Figure 5. Translation of CD79-CD22 bispecific activity from Fab-K$_D$-Fab to BYbe™. Fab-K$_D$-Fab and BYbe™ proteins were assessed in the B cell signaling assay. Bispecific BYbe™ proteins were tested alongside monospecific-monovalent BYbe™ proteins, monospecific-bivalent BYbe™ proteins and bivalent BYbe™ mixtures. For each molecule or mixture, 8-point concentration–response assays were performed in triplicate and pAkt, pp38, pPLCγ2 and pNF-κB levels were measured in B cells from the PBMC populations treated with anti-IgM. Percentage inhibition values relative to maximum and minimum control well data were calculated. Mean ± standard deviation of 4 donors are plotted.

mimic a T cell-dependent antigen response, B cells were costimulated with anti-IgM and anti-CD40 antibodies. Proliferation was measured after 5 d and the percentage inhibition of a given response was calculated for each molecule. B cell proliferation was inhibited by approximately 90% by the CD22-CD79 BYbe™ (Figure 6a) whilst little or no inhibition was observed with the negative or bivalent control BYbe™ molecules (<20%). The bivalent mixture of CD79-CD79 + CD22-CD22 BYbe™ proteins also failed to inhibit B cell proliferation, confirming that the CD22-CD79 molecule is an obligate bispecific, as the inhibitory function cannot be replicated by antibodies targeting either of the antigens alone or mixtures of these antibodies.

CD86 is upregulated on activated B cells and plays a crucial role in B-T cell cross-talk through interactions with CD28 and CTLA-4.[24] We therefore examined CD86 expression by flow cytometry. In parallel to inhibition of proliferation, CD86 expression was inhibited when cells were treated with the CD22-CD79 BYbe™ protein (>70%), but not with any of the bivalent BYbe™ proteins or the bivalent BYbe™ mixture (Figure 6b).

Inflammatory cytokines such as Lymphotoxin-α can be released by activated B cells. We therefore analyzed if the CD22-CD79 BYbe™ could also inhibit the release of such cytokines in comparison to bivalent BYbe™ proteins or the bivalent BYbe™ mixture. Purified B cells were stimulated with anti-IgM/G (to activate naïve and memory B cells) and anti-CD40 antibodies, and Lymphotoxin-α levels were measured after 3 d. We observed considerable inhibition of Lymphotoxin-α (>95%) with only the CD22-CD79 BYbe™ and none of the control molecules (Figure 6c). In addition, we confirmed that conversion of the CD22-CD79 Fab-K$_D$-Fab to a bispecific IgG antibody format still retained inhibition of cytokine release (>80%) compared to a negative control IgG (~10%) (Figure 6d). SE-UPLC data for purified IgG proteins are shown in Figure S2b.

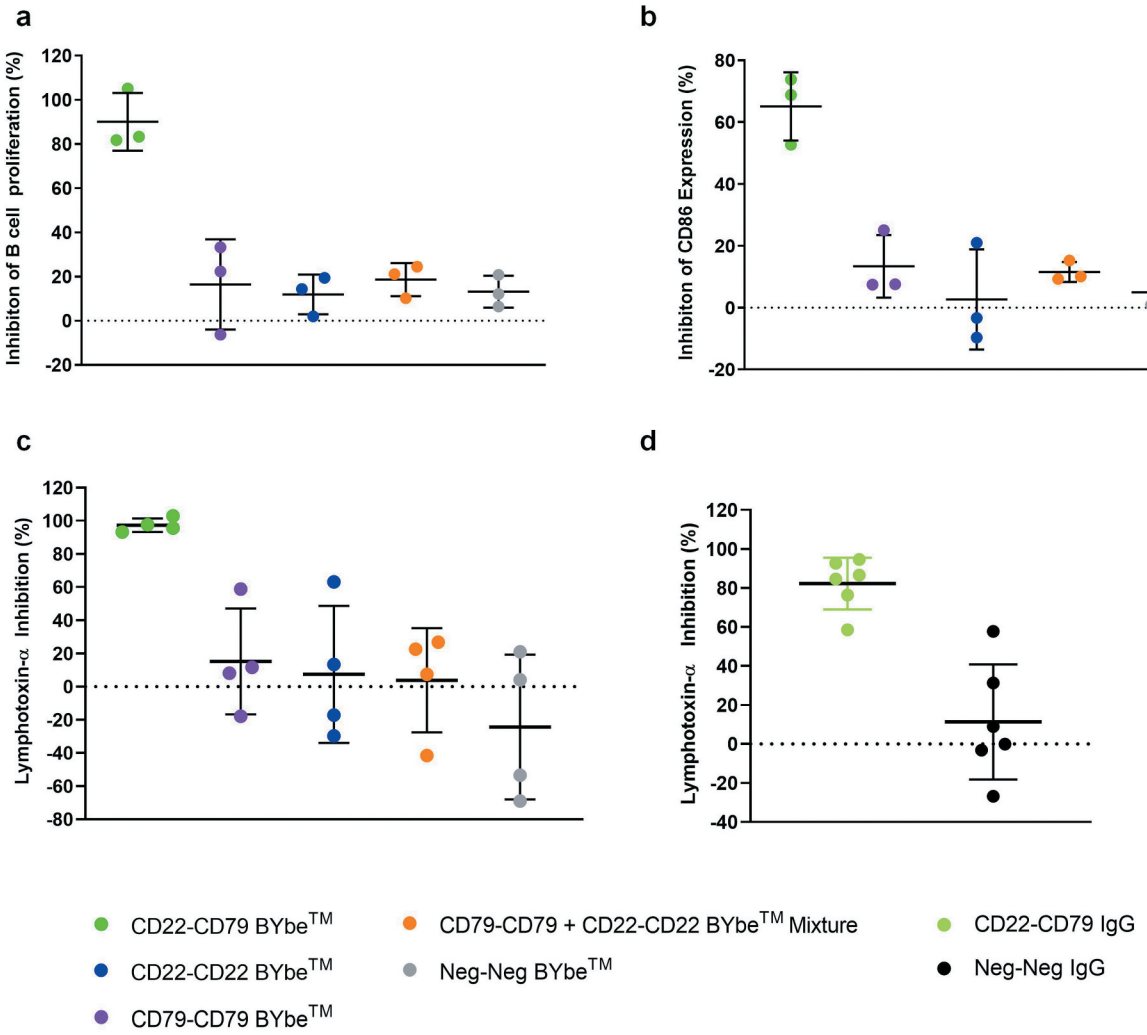

Figure 6. Inhibition of B cell functional responses with a CD22-CD79 bispecific BYbe™ and a CD22-CD79 bispecific IgG antibody. (a) Inhibition of B cell proliferation in CellTrace™ violet-labeled PBMC stimulated with anti-IgM and anti-CD40 antibodies ± test molecules (100 nM). (b) Inhibition of CD86 expression on B cells from CellTrace™ violet-labeled PBMC stimulated with anti-IgM and anti-CD40 antibodies ± test molecules (100 nM). In (a) and (b), inhibition was calculated relative to maximum (anti-IgM stimulation only) and minimum (no stimulation) controls. For each test condition, each dot represents the mean of triplicate wells from a single donor and a total of 3 donors are plotted. (c) BYbe™ protein activity in a cytokine release assay. (d) Bispecific IgG activity in a cytokine release assay. In (c) and (d), Lymphotoxin-α was measured following treatment of purified B cells stimulated with anti-IgM/G and anti-CD40 antibodies ± test molecules (100 nM). Percentage inhibition values relative to maximum and minimum controls were calculated. For each test condition each dot represents the mean of triplicate wells from a single donor and a total of either 4 (c) or 6 (d) donors are plotted. The solid horizontal lines represent the mean ± standard deviation.

Bispecific screen for inhibitors of ECM accumulation

In our second example, we sought to identify novel target combinations with potential anti-fibrotic activity. Fibrotic disease is thought to initiate with a chronic organ insult resulting in an inflammatory infiltrate of macrophages that release cytokines such as transforming growth factor-β; this induces the resident fibroblast population to proliferate and differentiate into myofibroblasts, which release an excess of ECM into the surrounding tissue.[25] This ECM protein accumulation is a hallmark of fibrosis and has been used to measure fibrotic disease in many different organ systems. We therefore developed an assay that mimicked this tissue remodeling, by assessment of ECM accumulation in the absence or presence of Fab-K_D-Fab proteins. The previously described high-content, high-throughput *in vitro* ECM kidney coculture assay[14,26] was modified to model ECM accumulation by lung-derived cells. ECM accumulation was measured in a 7 d coculture system of human primary lung fibroblasts and epithelial cells, whereby coculturing the two cell types resulted in spontaneous ECM accumulation. Three specific ECM components, fibronectin, collagen I and collagen III, were quantified.

To generate Fab-X and Fab-Y libraries, we selected 23 target antigens based on their known involvement in fibrotic mechanisms and expression level in the cells used in the coculture assay. Antibodies were made to a total of 23 different antigens, and between 1 and 5 unique V-regions were selected for screening based purely on their ability to bind the target antigen as a Fab-Y and originating from different V-region sequence families. Fab-X and Fab-Y antibodies covering these 23 unique antigens were purified and mixed to generate 1671 Fab-K_D-Fab molecules for screening. In total, bispecific antibodies encompassing 239 antigen combinations were screened. Two independent screens were performed with Fab-K_D-Fab

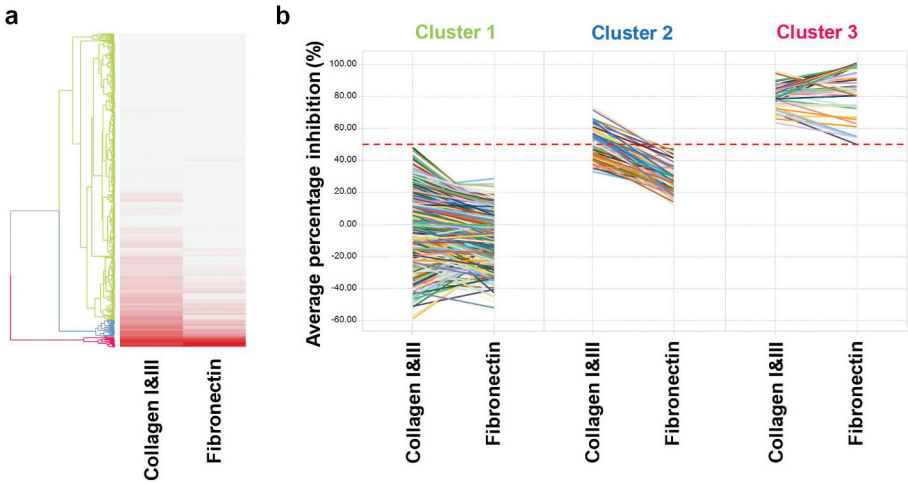

Figure 7. Identification of integrin αV-β1 and β1–β6 bispecific inhibitors of ECM accumulation from a phenotypic lung cell coculture screen. (a) UPGMA clustered heat map showing activity of Fab-K_D-Fab proteins tested at a single concentration (10 nM) on fibronectin and collagens I and III accumulation in the lung cell coculture assay. Gray denotes ≤0% inhibition, red denotes ≥100% inhibition of ECM accumulation. Each horizontal line represents a different Fab-K_D-Fab molecule. The cluster analysis was pruned to three clusters depicted in green (cluster 1), blue (cluster 2) and pink (cluster 3) on the dendrogram. (b) Average percentage inhibition of ECM deposition for all Fab-K_D-Fab molecules in each of the 3 clusters defined in the dendrogram. Red dashed line denotes 50% inhibition; this was the criteria for hit selection. The β1–β6 and αV-β1 target pairs were selected from the most inhibitory cluster (cluster 3). Each horizontal line represents a different Fab-K_D-Fab molecule.

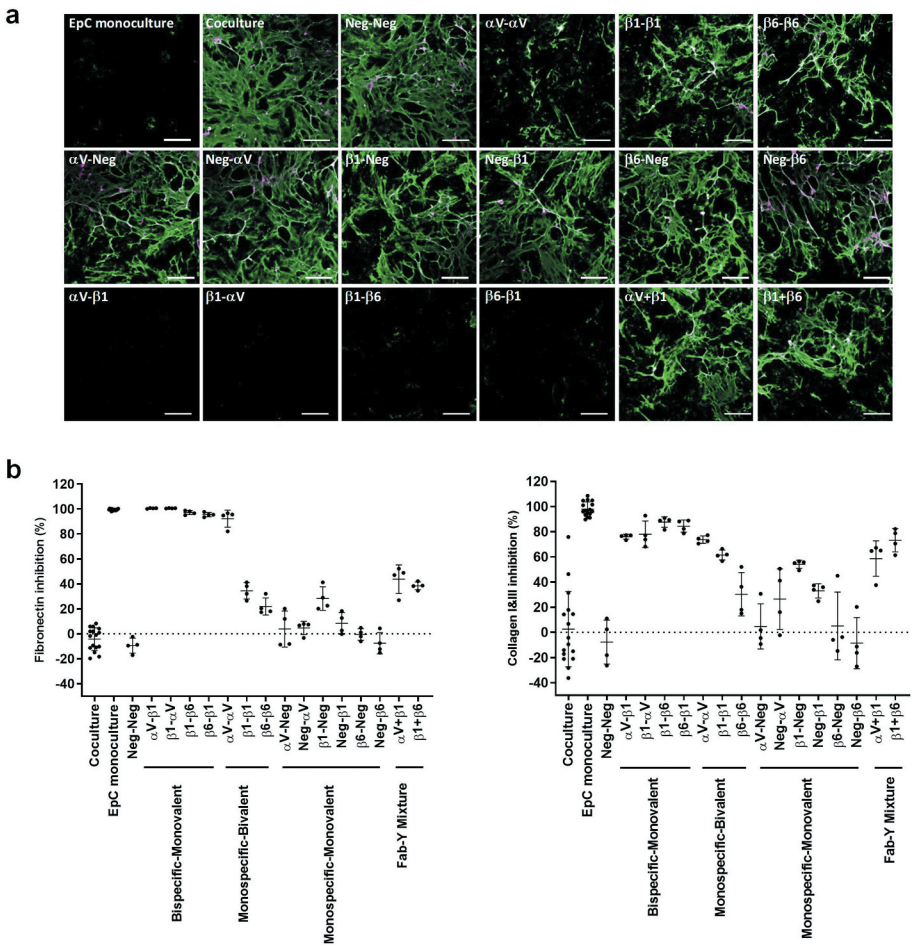

Figure 8. Validation of integrin αV-β1 and β1–β6 bispecific inhibitors of ECM accumulation from a phenotypic lung cell coculture screen. (a) SAEpC and IPF134 cell coculture induced matrix accumulation following treatment with 10 nM integrin β1–β6 or αV-β1 bispecific Fab-K_D-Fabs alongside monospecific-monovalent Fab-K_D-Fabs, monospecific-bivalent Fab-K_D-Fabs and Fab-Y mixtures. Images show fibronectin (green) and collagens I and III (magenta) staining by immunofluorescence; scale bar = 200 nm. (b) Assessment of integrin β1–β6 and αV-β1 bispecific Fab-K_D-Fabs alongside monospecific-monovalent Fab-K_D-Fabs, monospecific-bivalent Fab-K_D-Fabs and Fab-Y mixtures. Fab-K_D-Fabs were tested at 10 nM in quadruplicate, n = 2. Graphs show the percentage inhibition for fibronectin and collagens I and III. All data are plotted as mean ± standard deviation.

molecules tested at a final concentration of 10 nM. A heat map of the screen data was created using unweighted pair group method with arithmetic mean (UPGMA) hierarchical clustering,[27] which resulted in three discrete clusters of antigen combinations (Figure 7a). Primary screen hits were identified as those that induced more than or equal to 50% inhibition of fibronectin and collagen I and III in both screens; these were located in cluster 3 of the dendrogram (Figure 7b). This resulted in 28 hits, from which two lead antigen pairs that induced maximal inhibition of ECM accumulation were selected: β1–β6 (bispecific co-targeting integrins β1 and β6) and αV-β1 (bispecific co-targeting integrins αV and β1). From a total of 14 integrin β1–β6 bispecifics tested, comprising 4 different V-regions to integrin β1 and 4 different V-regions to integrin β6, only 3 resulted in more than 50% inhibition of both fibronectin and collagens I and III. A total of 23 integrin αV-β1 bispecifics were tested, comprising 6 different V-regions to integrin αV and 5 different V-regions to integrin β1, of which 12 resulted in greater than 50% inhibition of both fibronectin and collagens I and III.

β1–β6 and αV-β1 bispecific validation in the Fab-K_D-Fab format

To validate the primary hits identified in the ECM lung coculture assay, the integrin β1–β6 and αV-β1 Fab-K_D-Fab screen hits were assayed at a single concentration of 10 nM alongside monospecific-bivalent Fab-K_D-Fab controls, monospecific-monovalent Fab-K_D-Fab controls and Fab-Y mixtures. Accumulation of fibronectin and collagen I and III was quantified; representative images are shown in Figure 8a.

Integrin β1–β6 bispecific Fab-K_D-Fab molecules in both orientations, β1–β6 (β1 Fab-X-β6 Fab-Y) and β6-β1 (β6 Fab-X-β1 Fab-Y), induced considerable inhibition of fibronectin (96–97%) and collagen I and III (~85-88%) accumulation. The monospecific-bivalent Fab-K_D-Fab controls and monospecific-monovalent Fab-K_D-Fab and Fab-Y mixture controls showed limited inhibition of fibronectin deposition (<38%) in comparison (Figure 8b), demonstrating the obligate bispecific effect of the integrin β1–β6 pair with respect to inhibition of fibronectin accumulation. The effects of the control molecules were less clear-cut with respect to collagen I and III accumulation. The integrin β6-β6 bivalent Fab-K_D-Fab control and β6 monospecific-monovalent Fab-K_D-Fab control showed limited inhibition of collagen I and III accumulation (<30%). However, the equivalent controls containing only integrin β1 molecules showed up to 62% inhibition, with the β1 + β6 Fab-Y mixture showing approximately 73% inhibition of collagen I and III accumulation. Thus, with respect to inhibition of collagen I and III accumulation, this apparent additive effect was enhanced when the integrin β1 and β6 Fabs were physically linked in the bispecific Fab-K_D-Fab molecules.

Integrin αV-β1 bispecific Fab-K_D-Fab molecules in both orientations, αV-β1 (αV Fab-X-β1 Fab-Y) and β1-αV (β1 Fab-X-αV Fab-Y), also induced considerable inhibition of fibronectin (100–101%) and collagen I and III (76–78%) accumulation (Figure 8b). As expected from previous studies that showed inhibition of ECM accumulation with a bivalent anti-integrin αV antibody,[26,28] the bivalent αV-αV Fab-K_D-Fab also induced considerable inhibition of fibronectin (92%) and collagen I and III (74%) accumulation. The monospecific-monovalent Fab-K_D-Fab molecules showed modest inhibition (<30%) of ECM accumulation, and the αV + β1 Fab-Y mixture caused similar inhibition of fibronectin accumulation (44%) and enhanced inhibition of collagen I and III accumulation (59%), but the activity was markedly enhanced when the integrin αV and β1 Fabs were physically linked in the bispecific Fab-K_D-Fab molecules.

Overall, both the integrin β1–β6 and αV-β1 bispecific antibodies showed enhanced bispecific-dependent effects on ECM accumulation that ranged from obligate to additive activity depending on the target combination and on the respective ECM protein. Cell viability at the end of the assay was similar across all Fab-K_D-Fab treatment conditions compared to untreated coculture controls (Figure S4), indicating that the inhibition of ECM accumulation induced by the bispecific molecules was not due to direct effects on cell viability.

β1–β6 and αV-β1 bispecific validation in the BYbe™ format

The integrin β1–β6 and integrin αV-β1 target combinations identified in the single concentration ECM lung coculture bispecific screen were further validated in a concentration–response assay, measuring inhibition of fibronectin, collagen I and III accumulation after 7 d. The activity of the Fab-K_D-Fab bispecific was analyzed alongside the equivalent molecularly linked bispecific BYbe™ format, which contained either the αV or β6 specificity in the Fab position and β1 specificity in the scFv position. Bivalent BYbe™ antibodies that contained the same V-regions in both Fab and scFv positions were also included; BYbe™ schematics and SE-UPLC data for purified BYbe™ proteins are shown in Figure S2c. Similar concentration–response curves and IC_{50} values were obtained with Fab-K_D-Fab and BYbe™ bispecifics for both integrin β1–β6 (Figure 9a) and integrin αV-β1 bispecifics (Figure 9b), with the BYbe™ consistently demonstrating a moderate increase in potency compared to the Fab-K_D-Fab (Table S2). Moreover, the concentration–response data confirmed that both the integrin β1–β6 and integrin αV-β1 bispecific BYbe™ antibodies more potently inhibited both fibronectin and collagen I and III accumulation than the corresponding bivalent BYbe™ antibodies (integrin αV-αV, integrin β1–β1 and integrin β6–β6).

Bispecific screen for activators of T cell subsets

PBMC represent and cover the major leukocyte classes involved in both innate and adaptive immunity, apart from granulocytes. PBMC comprise a heterogenous population of cells that when manipulated *in vitro* provide a more physiologically relevant cellular environment compared to isolated component cell types, such as T cells, B cells and monocytes, that are no longer capable of responding to paracrine and autocrine signals provided by other cells. As such, identification of molecules modulating specific cell subsets within the wider PBMC population has increased translational potential to more complex biological systems. Screens can be adapted

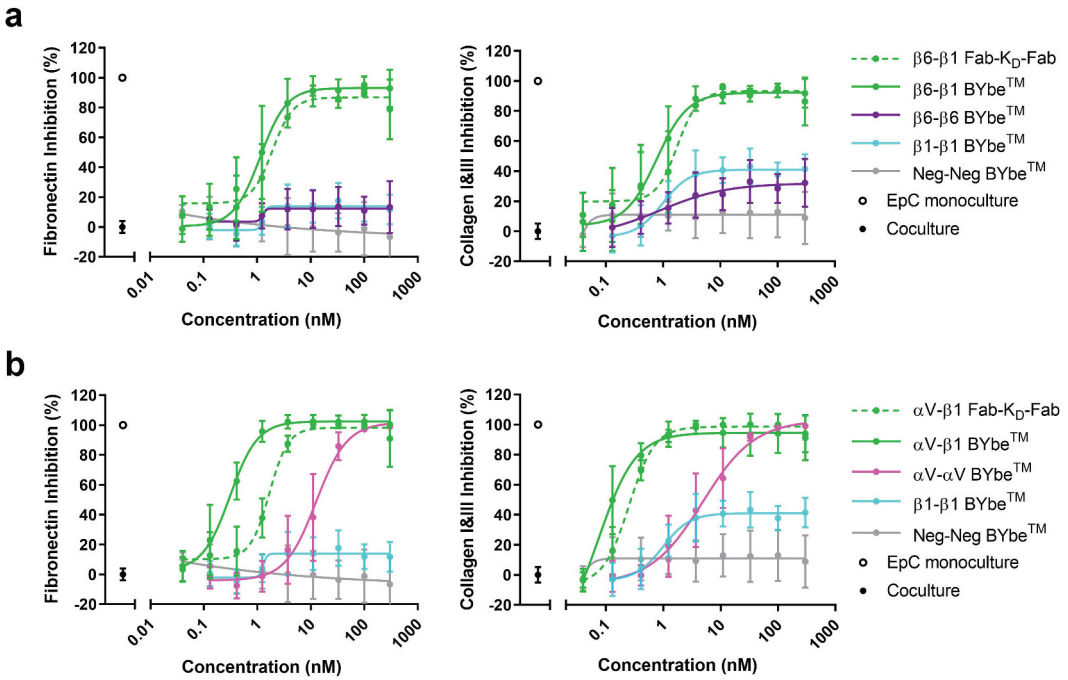

Figure 9. Translation of integrin β1–β6 and integrin αV-β1 bispecific activity from Fab-K$_D$-Fab to BYbe^{TM}. (a) Assessment of integrin β1–β6 Fab-K$_D$-Fab and BYbe^{TM} proteins in the lung cell coculture assay. (b) Assessment of integrin αV-β1 Fab-K$_D$-Fab and BYbe^{TM} proteins in the lung cell coculture assay. In (a) and (b), bispecific BYbe^{TM} proteins were tested alongside monospecific-bivalent BYbe^{TM} controls in a concentration–response assay measuring fibronectin and collagens I and III. Five biological replicates for each data point were tested and plotted as mean ± standard deviation.

specifically for different PBMC subsets of interest; however, here, we focused on identification of modulators of T cell activation.

In recent years, immunotherapy has become an established treatment option for an increasing number of cancer patients, exemplified by the increased use of therapeutic antibody-based immune checkpoint inhibitors (CPIs), including the now well-established CTLA-4 and PD-1-targeted biologics, ipilimumab, pembrolizumab and nivolumab.[29] Nevertheless, differences in efficacy across patient groups, ranging from complete responses to treatment relapse and even failure to respond,[30] imply that these mechanisms alone are insufficient. Hence, there is potential to identify novel modulators of T cell activation based on unbiased biology and novel bispecific target pairs to enhance T cell activation as additional or alternative treatments of cancer and infectious diseases.

We generated Fab-X and Fab-Y libraries targeting antigens that were selected based on their expression on T cells or other immune cells known to interact with T cells. Antibodies were made to a total of 49 different antigens and between 1 and 4 unique V-regions to each antigen were selected for screening from different V-region sequence families, based purely on their ability to bind PBMC as a Fab-Y. We deliberately did not pre-select antibodies of defined affinity, activity, or epitope to enable unbiased bispecific discovery, driven entirely by the functional cellular activity of the V-region combination. Fab-X and Fab-Y antibodies covering these 49 unique antigens were purified and mixed to generate 6417 Fab-K$_D$-Fab molecules for screening in a PBMC assay. In total, bispecific antibodies encompassing 969 antigen combinations were screened at 100 nM using PBMC from two independent donors. Cell activation was evaluated in unstimulated, anti-CD3-stimulated and Staphylococcal enterotoxin B (SEB)-stimulated culture conditions. The activation markers CD69, CD71, CD25 and CD137 were measured on seven different cell subsets in addition to quantification of the soluble mediators granzyme B, interferon (IFN)-γ and interleukin (IL)-2 in the conditioned medium. The cell subsets evaluated comprised both naïve and memory CD4 and CD8 T cells, monocytes, NK cells and B cells. This highly multiplexed screen format generated a large multidimensional dataset that we are currently evaluating using a range of analytical and informatics approaches. Examples of the diverse range of bispecific antibody activities identified are shown in Figure 10 using an interactive Spotfire® data visualization and mining tool that can be interrogated to query different phenotypic screen outputs, either one at a time or providing a global view of all bispecific antibodies in the screen. Example screening output heat maps for CD8 and CD4 T cell activation and a soluble mediator granzyme B are shown in Figure 10a-c; each square represents a different Fab-K$_D$-Fab molecule. Figure 10a shows expression of the activation marker CD137 on anti-CD3-stimulated CD8 T cells (both naïve and memory). Figure 10b shows expression of the activation marker CD25 on CD4 T cells (naïve and memory) stimulated with anti-CD3. Figure 10c shows modulation of granzyme B in SEB-stimulated PBMC. Activators of T cell activity are depicted in blue, whereas inhibitors of T cell activity are depicted in red. Bispecifics comprising a Fab-X targeting the costimulatory molecule CD28 or the canonical CPIs, PD-1 or CTLA-4, are highlighted to illustrate the diversity of activities observed with different Fab-K$_D$-Fab molecules and target combinations, though multiple novel T cell-activating target combinations beyond the PD-1 and CTLA-4 axis were also identified.

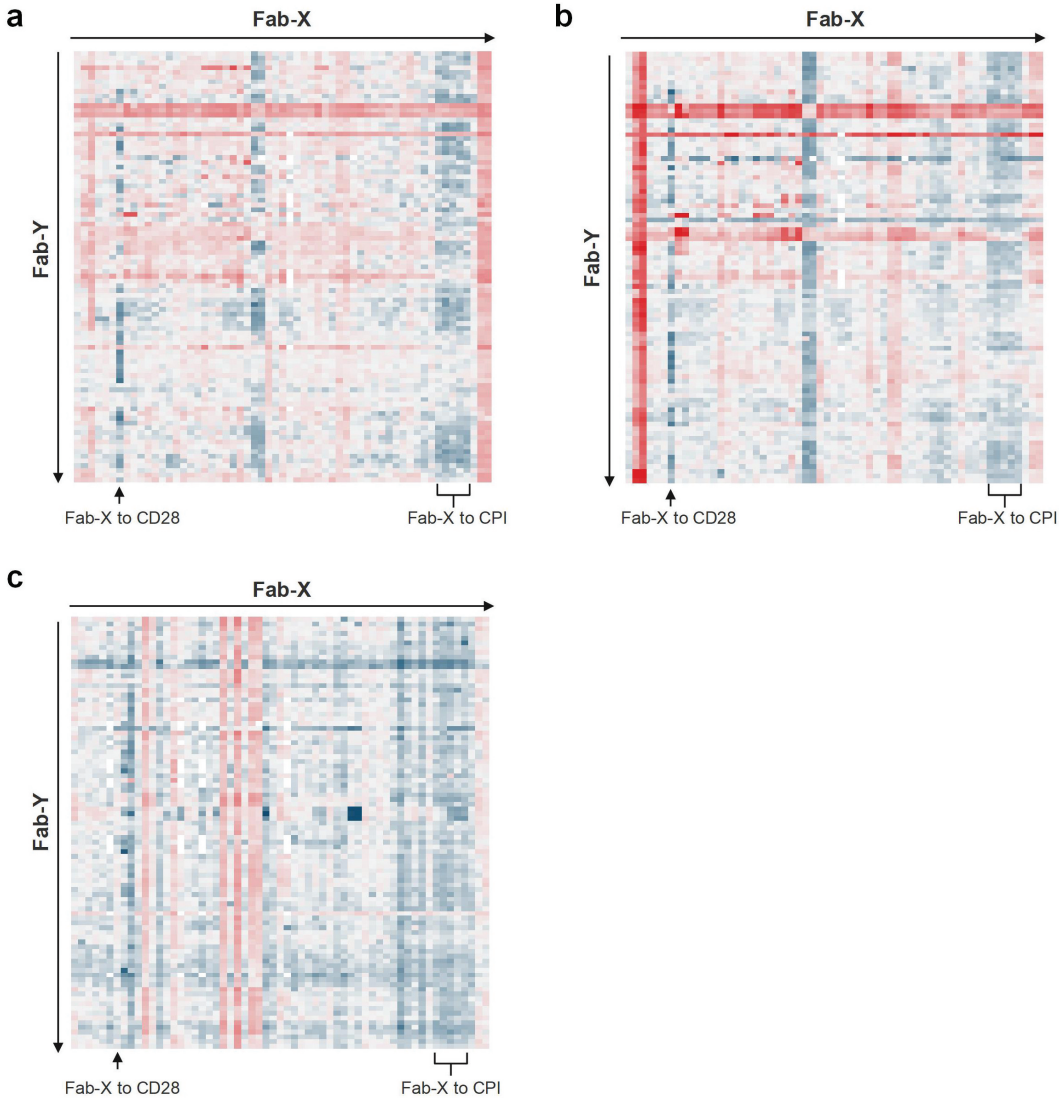

Figure 10. Identification of T cell activators and inhibitors from a stimulated PBMC screen. (a) Heat map of T cell screen data for Fab-K_D-Fab molecules tested in 2 donors at a single concentration (100 nM) in the T cell flow cytometry assay following anti-CD3 stimulation of PBMC. Log2 fold change of CD137 median fluorescence intensity relative to anti-CD3 stimulated untreated controls in CD8 T cells are depicted. (b) Heat map of T cell screen data for Fab-K_D-Fab molecules tested in 2 donors at a single concentration (100 nM) in the T cell flow cytometry assay following anti-CD3 stimulation of PBMC. Log2 fold change of CD25 median fluorescent intensity relative to anti-CD3 stimulated untreated controls in CD4 T cells are depicted. (c) Heat map of T cell screen data for Fab-K_D-Fab molecules tested in 2 donors at a single concentration (100 nM) in the PBMC soluble mediator assay following SEB stimulation of PBMC. Log2 fold change of the median fluorescent intensity of granzyme B detection beads relative to SEB-stimulated untreated controls are depicted. In (a) to (c), blue denotes an increase (max + 1.5 log2 fold change) and red denotes a reduction (max – 4.0 log2 fold change) in the readout stated, while gray denotes baseline. Data gaps are depicted in white. Each square represents a different Fab-K_D-Fab molecule.

Discussion

Bispecific antibodies can elicit novel biological functions that cannot be achieved with conventional monospecific antibodies, though novel bispecific target discovery remains a challenge. The functional activity of bispecific antibodies is not necessarily predicted from that of the parental antibodies. We thus propose that identification of the optimum target pair for modulation of a given disease phenotype is best achieved by high-throughput functional screening using diverse, combinatorial bispecific antibody libraries covering multiple targets. We describe here a novel *in vitro* combinatorial bispecific antibody format that enables rapid and efficient generation of large, high-quality bispecific antibody panels. We used these bispecific antibody panels in three high-throughput dual target discovery campaigns that incorporated distinct phenotypic screens to identify novel drug target pairs and bispecific antibodies for diverse disease indications.

Firstly, we developed a flow cytometry signaling assay using anti-IgM-stimulated PBMC to mimic the elevated B cell activation observed in SLE patients. Through screening 1992 bispecific antibodies encompassing 23 targets and 300 different antigen combinations, we identified a novel obligate bispecific BCR inhibitor co-targeting CD79a/b and CD22, which potently inhibited B cell activation. Activity of the identified CD79-CD22 target combination was entirely bispecific-dependent, with minimal activity being observed with the parental antibodies alone or mixtures of the two antibodies. CD22 is an inhibitory regulatory molecule recruited to the BCR following activation to limit the immune response and prevent

over-activation.[31] We speculate that the simultaneous physical co-engagement of CD22 with the positive signaling component of the BCR, CD79, by the bispecific antibody favors negative inhibitory signaling via CD22, thus overriding BCR activation via CD79.[32,33]

Secondly, we identified bispecifics co-targeting integrins β1 and β6 or αV and β1 as potent inhibitors of ECM accumulation from a longer-term high-content imaging assay from a screen containing 1671 bispecific antibodies encompassing 23 targets and 239 antigen combinations. These two novel bispecific target pairs displayed unique characteristics in the modulation of the ECM response over a 7 d assay period: the β1–β6 bispecific showed obligate inhibitory activity with respect to fibronectin accumulation and additive inhibitory activity with respect to collagen I and III accumulation; the bivalent αV-αV molecules were substantial inhibitors of ECM accumulation that could be enhanced further when paired with anti-β1 in the αV-β1 bispecific formats.

Thirdly, we introduced the concept of evaluating the modulation of multiple signaling pathways in diverse PBMC subsets in a single screen, combined with the ability to include different activating stimuli and markers for multiple cellular phenotypes. We demonstrated the ability to identify both activating and inhibitory bispecifics; in this case, identifying multiple activators as well as inhibitors of different T cell subsets. Validation of this unbiased screening approach was exemplified by the identification of several new target combinations with the reference costimulator CD28 and known CPIs such as PD-1 and CTLA-4, in addition to many additional novel non-predicted target pairs.

Across the three examples described, we screened thousands of bispecific antibodies to hundreds of antigen combinations to identify these novel bispecifics. High-throughput combinatorial target discovery on this scale has not been described to date, although unbiased bispecific functional screening has been reported to be necessary for identification of the optimal V-region pair.[8,9] We were able to generate sufficient numbers of bispecific antibodies at high purity for screening owing to the unique way in which our bispecific Fab-K_D-Fab antibody format is formed. Following *in vitro* mixing of the two component Fab-X and Fab-Y halves, the resulting bispecific complex is of sufficiently high purity and thus requires no further purification or processing prior to screening. Chemical conjugation techniques have historically been used to couple Fabs, but these methods still suffer from low yield and product heterogeneity.[34] Homogenous Fab conjugates have been generated by chemical conjugation of proteolytically cleaved IgGs, though reduction and oxidation in addition to multiple purification steps were required.[9] More recently, split protein reconstitution methods such as the SpyTag/SpyCatcher system have been used to covalently couple antibody fragments; however, SpyCatcher fusions can suffer from low expression[35] and multiple polishing steps are required to isolate homogeneous-ligated product.[36,37] Sortase-mediated covalent antibody conjugates have been successfully screened in biological assays without further purification of the conjugated product,[38] but certain assays may require removal of the sortase prior to screening. Combinatorial bispecific IgG libraries have also been generated by controlled Fab arm exchange, though removal of reducing agent is required following bispecific formation, and IgG bispecifics may be further hampered by restricted Fab arm geometry. The binding geometries of different IgG isotypes can vary dramatically, owing to differences in hinge sequences and flexibilities of Fab arms,[39] and this can manifest in vastly altered activities.[40] More importantly, activity from the Fc domain in IgG-based bispecifics may complicate the analysis of the effects of bispecific target engagement in cell assays utilizing immune cells. The Fab-K_D-Fab is therefore designed to be Fc-free for direct assessment of the effects of bispecific targeting, without interference from Fc-driven activity. Additional Fc function can be analyzed subsequently with selection of a wide choice of therapeutic bispecific antibody formats.[2] Importantly, in several examples, we showed that the functional activity of the Fab-K_D-Fab screening hits is verified in a molecularly linked therapeutically relevant antibody format. Fab-K_D-Fab activity was retained in a BYbe™ format,[16] which can subsequently be converted to a TrYbe™ therapeutic format[41] by the addition of an albumin-binding domain. We also demonstrated that the obligate CD79-CD22 bispecific activity was replicated in a full-length bispecific IgG format in a B cell cytokine release assay. The Fab-K_D-Fab target discovery format can thus reliably predict the effects of bispecific targeting in both Fab and scFv-based therapeutic antibody formats.

In summary, we have designed a unique bispecific screening format, that allows rapid generation of large numbers of high-quality bispecific antibodies to enable unbiased dual target identification by high-throughput functional screening in biologically relevant assays. Our *in vitro* combinatorial format technology can also be applied to smaller hypothesized screens for selection of optimal target pairs or V-region pairs for bispecific or biparatopic antibody development. V-regions suitable for expression as a Fab can be derived from any commonly used source, including immunizations or display libraries. Bispecific activity can also be assessed using Fab-K_D-Fab molecules generated from *in vitro* mixing of Fab-X and Fab-Y transiently expressing cell culture supernatants, without the need for purification, enabling even faster bispecific functional evaluation (data not shown). Our antibody library currently comprises approximately 1,500 purified Fab-X and Fab-Y molecules covering 150 different target specificities, with the potential to make approximately 450,000 unique Fab-K_D-Fab molecules by *in vitro* Fab-X and Fab-Y mixing. As well as bispecific Fab-K_D-Fab molecules, all the associated bivalent and single antigen-binding controls can also be easily made by combining the relevant component halves *in vitro*.

As the search for validated drug targets becomes increasingly challenging, phenotypic screening strategies are gaining momentum. Studies show that phenotypic drug discovery has been more successful in identifying small molecule drugs than target-based screening[42] and this target-agnostic approach is now being applied to monoclonal antibody drug discovery.[43] However, phenotypic screening with bispecific antibodies has been challenging owing to the difficulties in isolating the thousands of bispecific antibodies required at sufficient purity for screening. Our Fab-K_D-Fab format overcomes this hurdle, and our bispecific screening

platform can be applied to any disease area using translational human cell assays amenable to high-throughput screening. Our technology offers access to new or enhanced biology that cannot be attained with conventional antibodies, and thus provides a means to identify potentially first-in-class bispecific antibody therapeutics toward novel drug target pairings.

Materials and methods

Reagents

All materials, reagents and cell lines were sourced from Thermo Fisher Scientific unless otherwise stated.

Plasmid construction

The Fab-X and Fab-Y light chains were constructed as signal peptide-VL1-MsCκ for mouse- and human-derived V-regions, and signal peptide-VL1-MsCκ S171C for rabbit-derived V-regions, where VL1 is the variable light domain 1 and MsCκ is the mouse kappa light chain constant domain. The Fab-X heavy chain was constructed as signal peptide-VH1-MsCH1-Ala(Gly_4)-VL2-(Gly_4Ser)$_4$-VH2-10xHis-Myc, where VH1 is the variable heavy domain 1, MsCH1 is the mouse gamma-1 heavy chain CH1 constant domain, VL2 is the 52SR4 variable light domain and VH2 is the 52SR4 variable heavy domain.[17] 10xHis and Myc are C-terminal epitope tags. The Fab-Y heavy chain was constructed as signal peptide-VH1-MsCH1-Ala,Ser(Gly_4)-GCN4 peptide[17]-10xHis. The BYbe™ light chain was constructed as signal peptide-VL1-RbCκ, where VL1 is the variable light domain 1 and RbCκ is the rabbit kappa light chain constant domain. The BYbe™ heavy chain was constructed as signal peptide-VH1-RbCH1-Ser(Gly_4Ser)$_2$-VH2-(Gly_4Ser)$_4$-VL2 ± 6xHis, where VH1 is the variable heavy domain 1, RbCH1 is the rabbit gamma-1 heavy chain CH1 constant domain, VH2 is the variable heavy domain 2, VL2 is the variable light domain 2 and 6xHis is a C-terminal epitope tag. VL2 and VH2 in both Fab-X and BYbe™ heavy chains were disulfide stabilized, containing cysteines at VH44-VL100 (Kabat numbering), which is a disulfide bond location that is well tolerated among different scFv[44–46] and serves to prevent multimerization of Fab-X and BYbe™ proteins post-purification.[44] For full-length human IgG, light chain constructs comprised VL-hCκ S171C and heavy chain constructs comprised VH-hIgG4 containing S228P[47] and knobs-into-holes mutations.[48] Additional Fc null mutations, F234A and L235A, were incorporated to exclude the contributions of FcγR engagement in the cell assays.[49] All proteins were expressed from one of two closely related CMV-containing UCB-modified mammalian expression plasmids; pNAFL and pNAFH for light and heavy chains, respectively.

Antibody production

Antibody V-regions were derived from commonly used sources, such as rabbit and mouse immunization and subsequent B cell isolation,[50,51] bio-panning of naïve human antibody phage display libraries (reviewed by Hammers et al.[52]) or publicly available sequences. V-regions were ligated into Fab-X, Fab-Y, BYbe™[16] or knobs-into-holes IgG[48] expression plasmids using standard cloning methods. Expression plasmids were co-transfected into Expi293F™ cells using ExpiFectamine™ transfection kits or CHO-SXE cells[53] using ExpiCHO™ transfection kits according to the manufacturer's instructions. Cell culture supernatants were harvested by centrifugation and clarified 7–14 d post-transfection by passage through a 0.22-µm filter. Product concentration was determined by a protein G high-performance liquid chromatography (HPLC) assay by comparison of the A_{280} signal to a Fab standard. Fab-X and Fab-Y proteins were purified by one-step IMAC under endotoxin-free conditions using a vacuum-based purification system. Briefly, Ni^{2+}-sepharose resin was mixed with cell culture supernatant, packed into a column, washed with 50 mM Na_2PHO_4, 500 mM NaCl, pH 6.2 followed by 500 mM NaCl and eluted with 50 mM sodium acetate, 1 M NaCl, pH 4.0. Eluates were concentrated, buffer exchanged into phosphate-buffered saline (PBS), pH 7.4 and sterile filtered. BYbe™ proteins were purified from clarified cell culture supernatant by affinity chromatography followed by a preparative size exclusion polishing step. BYbe™ proteins with a 6xHis tag were IMAC purified, whereas untagged BYbe™ proteins were purified using Protein G. Briefly, tagged BYbe™ proteins were loaded onto a 5 mL Nickel HisTrap™ Excel column (GE Healthcare), then washed with 10 mM Na_2PHO_4, 500 mM NaCl, pH 7.4 followed by 10 mM Na_2PHO_4, 500 mM NaCl, 25 mM imidazole. Bound material was eluted with a 10 mM Na_2PHO_4, 500 mM NaCl, 250 mM imidazole, pH 7.4 step elution. Untagged BYbe™ proteins were loaded onto a Gammabind Plus Sepharose® XK26/20 column (GE Healthcare), washed with PBS, pH 7.4, eluted with a 100 mM glycine, pH 2.7 step elution and neutralized with 2 M Tris/HCl pH 8.5. Fractions containing BYbe™ proteins from the affinity capture step were pooled and concentrated using Amicon® Ultra centrifugal spin columns (Merck Millipore). Monomeric BYbe™ proteins were isolated by application onto a HiLoad® 16/60 Superdex® 200 column (GE Healthcare) equilibrated with PBS, pH 7.4. Fractions containing monomeric protein were pooled, sterile filtered and stored at 4°C. Parental IgG proteins were purified by flowing clarified supernatant over a 5 mL MabSelect SuRe™ column (GE Healthcare), which was washed with PBS, pH 7.4 prior to a 0.1 M sodium citrate, pH 3.6 step elution and neutralization with 2 M Tris/HCl, pH 8.5. Affinity purification was followed by a preparative gel filtration step using a Superdex® 200 10/300 GL column (GE Healthcare). Bispecific IgGs were generated by mixing relevant parental IgG molecules at a 1:1 molar ratio in the presence of 50 mM β-mercaptoethylamine overnight at 20°C. The mixtures were subjected to gel filtration and appropriate fractions were collected to isolate the final product in PBS, pH 7.4.

Antibody quality control

Purified antibodies were quantified by UV spectrophotometry using the Dropsense 96 (Trinean) or Cary 50 UV-Vis spectrophotometer (Agilent Technologies). Molecular weights were estimated by SDS-PAGE or capillary electrophoresis using the Labchip GXII Touch HT (Perkin Elmer) under reducing and non-reducing conditions, according to the manufacturer's instructions. NuPAGE® was performed on a Novex™ 4–20% Tris-glycine gel in Tris-Glycine SDS buffer according to the manufacturer's instructions. Purified protein samples (5 µg) contained 1× NuPAGE® LDS sample buffer and either 1× NuPAGE® sample reducing agent (reduced samples) or 10 mM N-Ethylmaleimide (non-reduced samples). SeeBlue™ Plus2 pre-stained protein standard was used as a molecular weight marker and protein bands were detected using InstantBlue® gel stain (Expedeon). Monomer level was determined by size exclusion ultra-performance liquid chromatography (SE-UPLC) or size exclusion HPLC. For SE-UPLC, 1 µg purified protein sample was injected onto an ACQUITY BEH200 column (Waters) and developed with an isocratic gradient of 200 mM sodium phosphate, pH 7.0 at 0.35 mL/min. Signal detection was by absorbance at 280 nm and multi-channel fluorescence. For SE-HPLC, 20 µg purified protein sample was injected onto a TSK Gel G3000SWXL, 7.8 × 300 mm column (Tosoh Bioscience) and developed with an isocratic gradient of 200 mM sodium phosphate, pH 7.0 at 1 mL/min. Signal detection was by absorbance at 280 nm. Gel filtration protein standards (BioRad) were loaded for molecular weight estimation. Since all purified Fab-X and BYbe™ proteins contained disulfide stabilized scFv, the observed monomer level is independent of protein concentration and unaffected by on-column dilution effects. Endotoxin was measured using the Endosafe® Portable Test System (Charles River) or the Limulus Amebocyte Lysate (LAL) chromogenic endotoxin quantification kit (Pierce), according to the manufacturer's instructions to ensure endotoxin levels of all antibodies were <1 EU/mg.

PBMC preparation

SLE donor PBMC were obtained from Tissue Solutions. Healthy volunteer PBMC were isolated from leukocyte cone blood (NHS Blood and Transplant Service) by density-gradient centrifugation in Leucosep™ tubes (Greiner-Bio-One). PBMC were frozen and stored in liquid nitrogen in accordance with UCB Celltech UK HTA License Number 12,504. Frozen PBMC were thawed, washed and resuspended in cell culture medium (RPMI 1640 medium supplemented with 10% (v/v) heat-inactivated fetal bovine serum, 100 U/mL Penicillin, 100 µg/mL Streptomycin and 2 mM Glutamax™) to the following densities: 3.33×10^6 cells/mL for SLE and healthy volunteer comparison assays, 1.25×10^6 cells/mL for primary screening and 5.00×10^6 cells/mL for concentration–response assays. Cell suspension (60 µL) was added to a v-bottomed 96-well polystyrene microtiter plate (VWR), which was sealed with a gas-porous adhesive cover and incubated at 37°C, 5% CO_2 for 60 min to allow the cells to acclimatize. For the B cell cytokine release assay, B cells were purified from PBMC by negative selection using the B cell Isolation Kit II (Miltenyi Biotec) to >95% purity by flow cytometry.

Intracellular B cell signaling analysis by flow cytometry

To generate Fab-K_D-Fabs, Fab-X and Fab-Y molecules were mixed in cell culture medium at an equimolar ratio and incubated for 1 h at 37°C. BYbe™ proteins were diluted in cell culture medium. Prepared Fab-K_D-Fab or BYbe™ proteins were incubated with acclimatized PBMC for 1 h. The cells were then stimulated via the BCR by addition of 25 µg/mL (final assay concentration) goat anti-human IgM antibody (Southern Biotech). Medium alone was added to non-stimulated cells. Cells were incubated at 37°C, 5% CO_2 for 15 min and then fixed with 100 µL/well BD Cytofix™ fixation buffer (BD Biosciences) at room temperature for 15 min. Cells were centrifuged at 500 × *g* for 5 min and the supernatant was removed. Plates were then vortexed and 100 µL/well ice-cold BD Permeabilization Buffer III (BD Biosciences) was added for 30 min. Cells were washed twice in flow buffer (PBS, pH 7.4 supplemented with 1% (w/v) BSA, 0.1% (v/v) NaN_3, 2 mM EDTA) using an ELX automated plate washer (BioTek). Cells were resuspended by vortexing before Phosflow™ antibody staining. For assays comparing healthy volunteer with SLE patient B cells, two different antibody panels (BD Biosciences) were used containing antibodies to B cell surface markers and phosphorylated NF-κB (pNF-κB), Akt (pAkt), p38 (pp38), Syk (pSyk) and Erk1/2 (pErk1/2). Panels consisted of either: CD20-Alexa Fluor® 647 (Cat. No. 558,054), pNF-κB p65 (pSer529)-Alexa Fluor® 488 (Cat. No. 558,421), pAkt (pSer473)-PE (Cat. No. 561,671) and pp38 MAPK (pThr180/Tyr182)-PerCP Cy5.5 (Cat. No. 560,406) antibodies or CD20-Alexa Fluor® 647 (Cat. No. 558,054), pSyk-Alexa Fluor® 488 (pY348) (Cat. No. 560,081) and pErk1/2 (pThr202/Tyr204)-PE (Cat. No. 561,991) antibodies. For assays utilizing Fab-K_D-Fab and BYbe™ molecules, the following antibody panels (BD Biosciences) were used: CD20-Alexa Fluor® 488 (Cat. No. 558,056), pp38 MAPK (pThr180/Tyr182)-Alexa Fluor® 647 (Cat. No. 562,066), pAkt (pSer473)-PE (Cat. No. 561,671) and cleaved PARP (Asp214)-BD Horizon™ BV421 (Cat. No. 564,129) or CD20-Alexa Fluor® 488 (Cat. No. 558,056), pNF-κB p65 (pSer529)-Alexa Fluor® 647 (Cat. No. 558,422), pPLCγ2 (pTyr759)-PE (Cat. No. 560,134) and cleaved PARP (Asp214)-BD Horizon™ BV421 (Cat. No. 564,129). Cells were stained at room temperature in the dark for 1 h and washed twice with flow buffer before acquiring on the iQue® Screener Plus flow cytometer (IntelliCyt®). Cell populations were identified using ForeCyt® software (version 6.3, IntelliCyt®) and fluorescence intensity staining values for each phosphorylated signaling protein were exported into Spotfire® (version 7.11.1, TIBCO®) and GraphPad Prism (version 8.1.1, GraphPad Software, Inc.) for analysis and visualization. For concentration–response assays, non-linear curve fitting was performed in GraphPad Prism (version 8.1.1, GraphPad Software, Inc.) where possible.

B cell proliferation assay

PBMC were labeled with 5 µM CellTrace™ violet and then washed and resuspended at 2.00×10^6 cells/mL in cell culture medium. Cells (100 µL/well) were added to round-bottomed 96-well plates containing a final concentration of 100 nM BYbe™ proteins across triplicate wells. B cells in the culture were then stimulated with 12 µg/mL anti-IgM (Jackson ImmunoResearch, Cat. No. 109–006-129) and 1 µg/mL anti-CD40 antibody (Biotechne, Cat. No. AF632) and plates were incubated at 37°C, 5% CO_2 for 5 d. Proliferation and activation of B cells was measured by flow cytometry using human CD3-FITC (UCHT-1), CD19-APC-Cy-7 (HIB19), CD20-PE (2H7) and CD86-APC (IT2.2) antibodies (Biolegend®). Proliferation of B cells ($CD3^-CD20^+CD19^+$) was measured by dilution of CellTrace™ violet relative to unstimulated cells. The activation of B cells was determined by CD86 mean fluorescence intensity. All samples were acquired on a fluorescence-activated cell sorting (FACS) Canto II flow cytometer (BD Biosciences) and files were analyzed using FlowJo™ software (version 10.1, Becton Dickinson).

B cell cytokine release assay

Isolated B cells were resuspended at 2.00×10^6 cells/mL in cell culture medium. The isolated cells (100 µL/well) were added to round-bottomed 96-well plates and BYbe™ proteins or bispecific IgG molecules (100 nM final concentration) were added across triplicate wells. B cells were stimulated with 12 µg/mL anti-IgM/G (Jackson ImmunoResearch) and 1 µg/mL anti-CD40 antibody (Biotechne) at 37°C, 5% CO_2 for 3 d. Conditioned medium was harvested from each well and Lymphotoxin-α was measured using a Lymphotoxin-α/TNF-β DuoSet® ELISA (Biotechne). Absorbance readings at 450 nm were measured on a Synergy Neo2 multi-mode microplate reader (BioTek) and data analyzed using GraphPad Prism software (version 8.1.1, GraphPad Software, Inc.).

Fibrosis assay cell preparation

Human small airway epithelial cells (SAEpC) (ATCC, PCS-301-010) were maintained in airway epithelial cell basal medium (ATCC) supplemented with bronchial epithelial cell growth kit (ATCC). Human primary lung fibroblasts derived from a patient with idiopathic pulmonary fibrosis (ATCC, CCL-134, IPF134) were cultured in fibroblast basal medium supplemented with FGM™-2 SingleQuots™ pack (Lonza). In the fibrosis assay screen, SAEpC and IPF134 cells were cocultured in a 1:1 ratio in renal epithelial cell basal medium (ATCC) supplemented with renal epithelial cell growth kit (ATCC). Cells were grown at 37°C, 5% CO_2.

Fibrosis screen assay

To generate Fab-K_D-Fabs, Fab-X and Fab-Y molecules were mixed in renal epithelial cell growth medium at an equimolar ratio and incubated for 1 h at 37°C. BYbe™ proteins were diluted in renal epithelial cell growth medium. Fab-K_D-Fab or BYbe™ proteins were added to 384-well black, clear bottom plates (Greiner Bio-One). Both SAEpC and IPF134 cell cultures were then added, seeded at a density of 2000 cells/well. SAEpC monocultures and untreated cocultures were included as controls. Plates were incubated at 37°C, 5% CO_2 for 7 d. Cell viability was assessed using PrestoBlue® cell viability reagent according to the manufacturer's instructions.

Immunofluorescence of ECM

Cells were washed in PBS, pH 7.4 and lysed with 250 mM NH_4OH in 25 mM Tris (Sigma-Aldrich) for 30 min at 37°C, 5% CO_2. ECM was washed three times in PBS, pH 7.4, fixed with 100% methanol for 30 min at −20°C, then washed 3 times in PBS, pH 7.4. Staining was performed with fibronectin-Alexa Fluor® 488 (eBioscience, clone FN-3) and collagen I and anti-collagen III (Millipore, AB745 and AB747) antibodies. Collagen I and III antibodies were detected using goat anti-rabbit IgG (H + L)-Alexa Fluor® 647 secondary antibodies. Plates were scanned on the ArrayScan HCS reader (Cellomics-Thermo) using a 10x objective (X1 camera) with 2 × 2 binning (1.104 x1.104 pixels/field). Four fields of view per well were collected.

High-content analysis of ECM

Image analysis of fibronectin and collagens I and III was conducted using Pipeline Pilot (version 9.2, Biovia). Size, shape, intensity, and texture statistics were collected from each raw image and averaged across the four fields collected for each well. A Pareto scale was then applied to each of the 64 collected statistics and positive (epithelial cell monoculture) and negative control wells (epithelial-fibroblast coculture) were then used to build a Partial Least Square (PLS) model using R software[54] for analysis. Test well statistics were then analyzed by the PLS model to generate a score which was multiplied by 100 to generate a percentage inhibition; 100 representing 100% inhibition of matrix accumulation, and 0 representing no inhibition of matrix accumulation as compared to controls on each plate. In this model it was possible to obtain negative values and values greater than 100 if there was increased or decreased fibronectin and/or collagen I and III in the treatment wells compared to the control wells, respectively. Data from Pipeline Pilot were exported into Spotfire® (version 7.11.1, TIBCO®) for visualization and analysis, or to GraphPad Prism (version 8.1.1, GraphPad Software, Inc.). In concentration–response assays, fibronectin, and collagen I and III fluorescence intensity measurements were taken from the "Cellomics Cell Health Profiling V4" bio-application. Non-linear curve fitting was performed in GraphPad Prism (version 8.1.1, GraphPad Software, Inc.) where possible.

T cell analysis by flow cytometry

To generate Fab-K_D-Fabs, Fab-X and Fab-Y molecules were mixed in TexMACs cell culture medium at an equimolar ratio and incubated for 1 h at 37°C. PBMC (1.00×10^5) were added to 384-well tissue culture plates, followed by addition of the Fab-K_D-Fab proteins. The cells were then activated via T cell receptor stimulation either by addition of 250 ng/mL (final

assay concentration) mouse anti-human CD3 (eBioscience, UCHT1) or 1 µg/mL (final assay concentration) SEB (Sigma-Aldrich). Medium alone was added to unstimulated cells. Cells were incubated at 37°C, 5% CO_2 for 48 h and then centrifuged at 500 × *g* for 5 min and the conditioned medium transferred to a storage plate and placed at −80°C. Cell plates were then washed twice in flow buffer using an ELX automated plate washer (BioTek). Cells were resuspended by vortexing prior to antibody staining. Antibody details are shown in Table S3. Cells were stained at 4°C in the dark for 45 min and washed twice with flow buffer before fixing in BD CellFix overnight. The plates were then centrifuged at 500 × *g* for 5 min, the supernatant was removed, and the pellet resuspended in FACS buffer before acquiring on the iQue® Screener Plus flow cytometer (IntelliCyt®). ForeCyt® software (version 6.3, IntelliCyt®) was used to gate on CD14+ monocytes, CD56 + NK cells, CD19+ B-cells, CD4+ and CD8+ memory and naïve T cells. For each cell population, the cellular expression of CD69, CD25, CD71 and CD137 was measured as reported median fluorescence intensity values. The data were then used to calculate the log2 fold changes in expression relative to control well values and exported into Spotfire® (version 7.11.1, TIBCO®) for analysis and visualization.

PBMC soluble mediator analysis

Conditioned medium was quantified for granzyme B, IFNγ and IL-2 using the IntelliCyt® QBead PlexScreen kit. The conditioned medium was removed from −80°C storage and allowed to thaw. Plates stimulated with either anti-CD3 or SEB were diluted 1 in 20 in TexMACs media, while unstimulated plates were diluted 1 in 5. The samples were then added to plates containing analyte-specific capture beads. The plates were vortexed and incubated at room temperature in the dark for 1 h. The detection antibodies were added to the wells and the plates vortexed and incubated for a further 2 h. Wash buffer was then added before centrifugation at 1100 × *g* for 5 min. The supernatant was removed using an ELX automated plate washer (BioTek) and the beads resuspended by vortexing before acquisition on the iQue® Screener. Bead populations were identified using ForeCyt® software (version 6.3, IntelliCyt®) and median fluorescence intensity staining values for each population were generated. The data were then used to calculate the log2 fold changes in expression relative to control well values and exported into Spotfire® (version 7.11.1, TIBCO®) for analysis and visualization.

Statistics and reproducibility

Experiments analyzing BCR activity in healthy versus SLE patient samples were performed with n = 12 donors and three technical replicates per donor. Geometric mean fluorescence values of intracellular phosphorylated protein expression were calculated for each activation readout. *p*-Values were determined by a two-tailed unpaired *t*-test.

Abbreviations

BCR	B cell receptor
BiTE	Bispecific T cell engager
CMV	Cytomegalovirus
CPI	Checkpoint inhibitor
ECM	Extracellular matrix
EDTA	Ethylenediaminetetraacetic acid
ELISA	Enzyme-linked immunosorbent assay
Fab	Antigen-binding fragment
Fab-X	Fab-52SR4 scFv fusion
Fab-Y	Fab-GCN4 peptide fusion
Fab-K_D-Fab	Fab-X:Fab-Y bispecific complex
FACS	Fluorescence-activated cell sorting
Fc	Fragment crystallizable region
G4S	Gly_4Ser
HCS	High-content screen
HPLC	High-performance liquid chromatography
IgG	Immunoglobulin G
IgM	Immunoglobulin M
IMAC	Immobilized metal affinity chromatography
NK	Natural killer
pAkt	Phosphorylated Akt
PBMC	Peripheral blood mononuclear cells
PBS	Phosphate-buffered saline
pErk1/2	Phosphorylated Erk1/2
PLS	Partial least square
pNF-κB	Phosphorylated NF-κB
pp38	Phosphorylated p38
pPLCγ2	Phosphorylated PLCγ2
pSyk	Phosphorylated Syk
SAEpC	Human small airway epithelial cells
scFv	Single-chain variable fragment
SDS-PAGE	Sodium dodecyl sulfate–polyacrylamide gel electrophoresis
SE	Size exclusion
SEB	Staphylococcal enterotoxin B
SLE	Systemic lupus erythematosus
TNF	Tumor necrosis factor
UPGMA	Unweighted pair group method with arithmetic mean
UPLC	Ultra-performance liquid chromatography
V-region	Variable region

Acknowledgments

The authors would like to thank: Michael Wright for Fab-X and Fab-Y format design, Matthew Page for B cell screen analysis, Helene Bon for ECM assay development, Ross Paveley for high-content image analysis development, Camilla Pang for data visualization, Halima Aliyu for ECM screen immunofluorescence staining and the Antibody Discovery and Antibody Production groups for their help with antibody library production. The authors would also like to thank Alastair Lawson, David Humphreys, Sam Heywood and Andy Popplewell for proofreading the manuscript and Neil Weir for his belief in this technology and support to develop the platform.

Author Contributions

P.B., K.D.W., C.L.T., A.K.S., D.A.C., M.M., L.E.S., E.M.C.B. and S.J. P. designed and carried out experiments, analyzed and interpreted data and contributed to writing the manuscript. A.M.K. analyzed and interpreted data and contributed to writing the manuscript. B.M.T. contributed to the concept of the work, designed experiments, interpreted data, and contributed to writing the manuscript. H.M.F and S.E.R. contributed to the concept of the work, designed and carried out experiments, analyzed and interpreted data and contributed to writing the manuscript.

Data Availability

All data generated or analyzed to support the conclusions drawn in this study are included in this published article (and its supplementary information files).

Disclosure of interest

All authors are employees and P.B., H.M.F., K.D.W., A.K.S., S.E.R., L.E.S., B.M.T., S.J.P. and A.M.K. are shareholders of UCB Pharma. Patents US10358493B2, WO2016/009030, US7993864B2 and EP1570267B1 cover the technology described in this manuscript.

Disclosure statement

No potential conflict of interest was reported by the authors.

References

1. Kaplon H, Muralidharan M, Schneider Z, Reichert JM. Antibodies to watch in 2020. MAbs. 2020;12(1):1703531. doi:10.1080/19420862.2019.1703531.
2. Brinkmann U, Kontermann RE. The making of bispecific antibodies. MAbs. 2017;9(2):182–212. doi:10.1080/19420862.2016.1268307.
3. Lillicrap D. Bispecific antibody therapy in hemophilia. N Engl J Med. 2017;377(9):884–85. doi:10.1056/NEJMe1707802.
4. Gokbuget N, Dombret H, Bonifacio M, Reichle A, Graux C, Faul C, Diedrich H, Topp MS, Bruggemann M, Horst HA, et al. Blinatumomab for minimal residual disease in adults with B-cell precursor acute lymphoblastic leukemia. Blood. 2018;131(14):1522–31. doi:10.1182/blood-2017-08-798322.
5. Kantarjian H, Stein A, Gökbuget N, Fielding AK, Schuh AC, Ribera J-M, Wei A, Dombret H, Foà R, Bassan R, et al. Blinatumomab versus chemotherapy for advanced acute lymphoblastic leukemia. N Engl J Med. 2017;376(9):836–47. doi:10.1056/NEJMoa1609783.
6. Ellerman D. Bispecific T-cell engagers: towards understanding variables influencing the in vitro potency and tumor selectivity and their modulation to enhance their efficacy and safety. Methods. 2019;154:102–17. doi:10.1016/j.ymeth.2018.10.026.
7. Labrijn AF, Janmaat ML, Reichert JM, Parren PWHI. Bispecific antibodies: a mechanistic review of the pipeline. Nat Rev Drug Discovery. 2019;18:585–608.
8. Geuijen CAW, De Nardis C, Maussang D, Rovers E, Gallenne T, Hendriks LJA, Visser T, Nijhuis R, Logtenberg T, de Kruif J, et al. Unbiased combinatorial screening identifies a bispecific igG1 that potently inhibits HER3 signaling via HER2-guided ligand blockade. Cancer Cell. 2018;33(5):e910. doi:10.1016/j.ccell.2018.04.003.
9. Patke S, Li J, Wang P, Slaga D, Johnston J, Bhakta S, Panowski S, Sun LL, Junttila T, Scheer JM, et alA. bisFabs: tools for rapidly screening hybridoma IgGs for their activities as bispecific antibodies. MAbs. 2017;9(3):430–37. doi:10.1080/19420862.2017.1281504.
10. Jost C, Schilling J, Tamaskovic R, Schwill M, Honegger A, Pluckthun A. Structural basis for eliciting a cytotoxic effect in HER2-overexpressing cancer cells via binding to the extracellular domain of HER2. Structure. 2013;21(11):1979–91. doi:10.1016/j.str.2013.08.020.
11. White AL, Chan HT, French RR, Willoughby J, Mockridge CI, Roghanian A, Penfold CA, Booth SG, Dodhy A, Polak ME. Conformation of the human immunoglobulin G2 hinge imparts superagonistic properties to immunostimulatory anticancer antibodies. Cancer Cell. 2015;27(1):138–48. doi:10.1016/j.ccell.2014.11.001.
12. Moraga I, Wernig G, Wilmes S, Gryshkova V, Richter CP, Hong WJ, Sinha R, Guo F, Fabionar H, Wehrman TS. Tuning cytokine receptor signaling by re-orienting dimer geometry with surrogate ligands. Cell. 2015;160(6):1196–208. doi:10.1016/j.cell.2015.02.011.
13. Musette P, Bouaziz JD. B cell modulation strategies in autoimmune diseases: new concepts. Front Immunol. 2018;9:622. doi:10.3389/fimmu.2018.00622.
14. Qureshi OS, Bon H, Twomey B, Holdsworth G, Ford K, Bergin M, Huang L, Muzylak M, Healy LJ, Hurdowar V. An immunofluorescence assay for extracellular matrix components highlights the role of epithelial cells in producing a stable, fibrillar extracellular matrix. Biol Open. 2017;6(10):1423–33. doi:10.1242/bio.025866.
15. Holdsworth G, Bon H, Bergin M, Qureshi O, Paveley R, Atkinson J, Huang L, Tewari R, Twomey B, Johnson T. Quantitative and organisational changes in mature extracellular matrix revealed through high-content imaging of total protein fluorescently stained in situ. Sci Rep. 2017;7(1):9963. doi:10.1038/s41598-017-10298-x.
16. Bhatta P, Davé E, Heywood SP, Humphreys DP, Smith BJ. Anti-fcrn antibodies. Ucb Pharma S A. 2016;WO16180765.
17. Zahnd C, Spinelli S, Luginbuhl B, Amstutz P, Cambillau C, Pluckthun A. Directed in vitro evolution and crystallographic analysis of a peptide-binding single chain antibody fragment (scFv) with low picomolar affinity. J Biol Chem. 2004;279(18):18870–77. doi:10.1074/jbc.M309169200.
18. Harwood NE, Batista FD. Early events in B cell activation. Annu Rev Immunol. 2010;28(1):185–210. doi:10.1146/annurev-immunol-030409-101216.
19. Kwak K, Akkaya M, Pierce SK. B cell signaling in context. Nat Immunol. 2019;20(8):963–69. doi:10.1038/s41590-019-0427-9.
20. Hashimoto A, Okada H, Jiang A, Kurosaki M, Greenberg S, Clark EA, Kurosaki T. Involvement of guanosine triphosphatases and phospholipase C-gamma2 in extracellular signal-regulated kinase, c-Jun NH2-terminal kinase, and p38 mitogen-activated protein kinase activation by the B cell antigen receptor. J Exp Med. 1998;188(7):1287–95. doi:10.1084/jem.188.7.1287.
21. Rawlings DJ, Metzler G, Wray-Dutra M, Jackson SW. Altered B cell signalling in autoimmunity. Nat Rev Immunol. 2017;17:421–36.
22. Ward J, J. H. Hierarchical grouping to optimize an objective function. J Am Stat Assoc. 1963;58(301):236–44. doi:10.1080/01621459.1963.10500845.
23. Nakamura T, Sekar MC, Kubagawa H, Cooper MD. Signal transduction in human B cells initiated via ig β ligation. Int Immunol. 1993;5(10):1309–15. doi:10.1093/intimm/5.10.1309.
24. Hathcock KS, Laszlo G, Pucillo C, Linsley P, Hodes RJ. Comparative analysis of B7-1 and B7-2 costimulatory ligands: expression and function. J Exp Med. 1994;180(2):631–40. doi:10.1084/jem.180.2.631.
25. Duffield JS, Lupher M, Thannickal VJ, Wynn TA. Host responses in tissue repair and fibrosis. Annu Rev Pathol. 2013;8(1):241–76. doi:10.1146/annurev-pathol-020712-163930.
26. Bon H, Hales P, Lumb S, Holdsworth G, Johnson T, Qureshi O, Twomey BM. Spontaneous extracellular matrix accumulation in a human in vitro model of renal fibrosis is mediated by αV integrins. Nephron. 2019;142(4):328–50. doi:10.1159/000499506.
27. Michener CD, Sokal RR. A quantitative approach to a problem in classification. Evolution: International Journal of Organic Evolution. 1957;11(2):130–62. doi:10.1111/j.1558-5646.1957.tb02884.x.
28. Henderson NC, Arnold TD, Katamura Y, Giacomini MM, Rodriguez JD, McCarty JH, Pellicoro A, Raschperger E, Betsholtz C, Ruminski PG, et al. Targeting of αv integrin identifies a core molecular pathway that regulates fibrosis in several organs. Nat Med. 2013;19(12):1617–24. doi:10.1038/nm.3282.
29. Hargadon KM, Johnson CE, Williams CJ. Immune checkpoint blockade therapy for cancer: an overview of FDA-approved

immune checkpoint inhibitors. Int Immunopharmacol. 2018;62:29–39. doi:10.1016/j.intimp.2018.06.001.
30. Haslam A, Prasad V. Estimation of the percentage of US patients with cancer who are eligible for and respond to checkpoint inhibitor immunotherapy drugs. JAMA Netw Open. 2019;2(5):e192535. doi:10.1001/jamanetworkopen.2019.2535.
31. Kelm S, Gerlach J, Brossmer R, Danzer C-P, Nitschke L. The ligand-binding domain of CD22 is needed for inhibition of the B cell receptor signal, as demonstrated by a novel human CD22-specific inhibitor compound. J Exp Med. 2002;195(9):1207–13. doi:10.1084/jem.20011783.
32. Hombach J, Tsubata T, Leclercq L, Stappert H, Reth M. Molecular components of the B-cell antigen receptor complex of the IgM class. Nature. 1990;343(6260):760–62. doi:10.1038/343760a0.
33. Kraus M, Alimzhanov MB, Rajewsky N, Rajewsky K. Survival of resting mature B lymphocytes depends on BCR signaling via the Igalpha/beta heterodimer. Cell. 2004;117(6):787–800. doi:10.1016/j.cell.2004.05.014.
34. Brennan M, Davison PF, Paulus H. Preparation of bispecific antibodies by chemical recombination of monoclonal immunoglobulin G1 fragments. Science. 1985;229(4708):81–83. doi:10.1126/science.3925553.
35. Reddington SC, Howarth M. Secrets of a covalent interaction for biomaterials and biotechnology: spyTag and spycatcher. Curr Opin Chem Biol. 2015;29:94–99. doi:10.1016/j.cbpa.2015.10.002.
36. Alam MK, Gonzalez C, Hill W, El-Sayed A, Fonge H, Barreto K, Geyer CR. Synthetic modular antibody construction by using the spytag/spycatcher protein-ligase system. Chembiochem. 2017;18(22):2217–21. doi:10.1002/cbic.201700411.
37. Hofmann T, Schmidt J, Ciesielski E, Becker S, Rysiok T, Schutte M, Toleikis L, Kolmar H, Doerner A. Intein mediated high throughput screening for bispecific antibodies. MAbs. 2020;12(1):1731938. doi:10.1080/19420862.2020.1731938.
38. Andres F, Schwill M, Boersma YL, Pluckthun A. High-throughput generation of bispecific binding proteins by sortase A-mediated coupling for direct functional screening in cell culture. Mol Cancer Ther. 2019;19(4):1080–88. doi:10.1158/1535-7163.MCT-19-0633.
39. Roux KH, Strelets L, Michaelsen TE. Flexibility of human IgG subclasses. J Immunol. 1997;159:3372–82.
40. Bournazos S, Gazumyan A, Seaman MS, Nussenzweig MC, Ravetch JV. Bispecific anti-HIV-1 antibodies with enhanced breadth and potency. Cell. 2016;165(7):1609–20. doi:10.1016/j.cell.2016.04.050.
41. Adams R, Bhatta P, Davé E, Heywood SP, Humphreys DP, Marshall D, Shaw SG, Lightwood DJ. Multi-specific antibody molecules having specificity for TNF-alpha, IL-17A and IL-17F. Ucb Pharma S A. 2017;WO17102830.
42. Zheng W, Thorne N, McKew JC. Phenotypic screens as a renewed approach for drug discovery. Drug Discov Today. 2013;18(21–-22):1067–73. doi:10.1016/j.drudis.2013.07.001.
43. Minter RR, Sandercock AM, Rust SJ. Phenotypic screening-the fast track to novel antibody discovery. Drug Discov Today Technol. 2017;23:83–90. doi:10.1016/j.ddtec.2017.03.004.
44. Weatherill EE, Cain KL, Heywood SP, Compson JE, Heads JT, Adams R, Humphreys DP. Towards a universal disulphide stabilised single chain fv format: importance of interchain disulphide bond location and vL-vH orientation. Protein Eng Des Sel. 2012;25(7):321–29. doi:10.1093/protein/gzs021.
45. Michaelson JS, Demarest SJ, Miller B, Amatucci A, Snyder WB, Wu X, Huang F, Phan S, Gao S, Doern A, et al. Anti-tumor activity of stability-engineered igG-like bispecific antibodies targeting TRAIL-R2 and LTbetaR. MAbs. 2009;1(2):128–41. doi:10.4161/mabs.1.2.7631.
46. Reiter Y, Brinkmann U, Kreitman RJ, Jung SH, Lee B, Pastan I. Stabilization of the Fv fragments in recombinant immunotoxins by disulfide bonds engineered into conserved framework regions. Biochemistry. 1994;33(18):5451–59. doi:10.1021/bi00184a014.
47. Angal S, King DJ, Bodmer MW, Turner A, Lawson AD, Roberts G, Pedley B, Adair JR. A single amino acid substitution abolishes the heterogeneity of chimeric mouse/human (IGG4) antibody. Mol Immunol. 1993;30(1):105–08. doi:10.1016/0161-5890(93)90432-B.
48. Atwell S, Ridgway JB, Wells JA, Carter P. Stable heterodimers from remodeling the domain interface of a homodimer using a phage display library. J Mol Biol. 1997;270(1):26–35. doi:10.1006/jmbi.1997.1116.
49. Alegre ML, Peterson LJ, Xu D, Sattar HA, Jeyarajah DR, Kowalkowski K, Thistlethwaite JR, Zivin, RA, Jolliffe L, Bluestone JA. A non-activating "humanized" anti-CD3 monoclonal antibody retains immunosuppressive properties in vivo. Transplantation. 1994;57(11):1537–43. doi:10.1097/00007890-199457110-00001.
50. Clargo AM, Goswami S, Hutchinson R, Kwong ZW, Yang J, Wang X, Yao Z, Sreedhara A, Cano T, Tesar D, et al. The rapid generation of recombinant functional monoclonal antibodies from individual, antigen-specific bone marrow-derived plasma cells isolated using a novel fluorescence-based method. MAbs. 2014;6(1):143–59. doi:10.4161/mabs.27044.
51. Tickle S, Howells L, O'Dowd V, Starkie D, Whale K, Saunders M, Lee D, Lightwood D. A fully automated primary screening system for the discovery of therapeutic antibodies directly from B cells. J Biomol Screen. 2015;20(4):492–97. doi:10.1177/1087057114564760.
52. Hammers CM, Stanley JR. Antibody phage display: technique and applications. J Invest Dermatol. 2014;134(2):1–5. doi:10.1038/jid.2013.521.
53. Cain K, Peters S, Hailu H, Sweeney B, Stephens P, Heads J, Sarkar K, Ventom A, Page C, Dickson A. A CHO cell line engineered to express XBP1 and ERO1-Lα has increased levels of transient protein expression. Biotechnol Prog. 2013;29(3):697–706. doi:10.1002/btpr.1693.
54. R Core Team. R: A language and environment for statistical computing. R Foundation for Statistical Computing, Vienna, Austria. 2014. https://www.r-project.org/